Evaluation of the MF-Tyre/MF-Swift 6.0 tyre model

H.E. Schouten

DCT 2005.126

Traineeship report

Supervisors: Monika Mössner-Beigel (DaimlerChrysler AG)
dr. ir. I.J.M. Besselink

Technische Universiteit Eindhoven
Department Mechanical Engineering
Dynamics and Control Group

Eindhoven, November, 2005

Summary

In this internship the MF-Tyre/MF-Swift 6.0 tyre model is coupled to a custom version of DADS. Therefore some settings needed to be changed and a special makefile was needed.

Within the TMPT-Benchmark a Continental tyre is considered and for this tyre TNO has parameterized their tyre model. Alternative tests were done at a different testrig. To study the predictive behavior of the tyre model, simulations with the tyre model were compared with the alternative measurements. There are several differences between the simulations and the alternative measurements.

First, the difference in the test rig results in several deviations. It is shown that increasing the cornering stiffness of the model by changing the scaling factor LKY results in a better match with the measurements.

Second, the MF-Tyre/MF-Swift model is capable of making very good fits on measurements, so it is important to have a good base of measurements. The area, where no measurements have taken place, has to be checked carefully!

Third, in the dynamic tests, the vertical force matches usually well, but the maximum of the longitudinal force was in all cleat tests too high. This is a known phenomenon of the MF-Tyre/MF-Swift model.

And finally, the frequency of the simulations was too high. Including the test rig dynamics in the simulations will result in a better match of the frequency.

Samenvatting

In deze stage is het bandmodel MF-Tyre/MF-Swift 6.0 gekoppeld aan een speciale versie van DADS. Daarvoor moesten enkele instellingen veranderd worden en een speciale makefile gemaakt worden.

Als onderdeel van de TMPT-Benchmark is een Continental band getest en heeft TNO de modelparameters bepaald. Daarnaast heeft DaimlerChrysler alternatieve testen uit laten voeren. In deze stage zijn simulaties uitgevoerd met het bandmodel en deze worden vergeleken met de alternatieve testen. Er zijn meerdere verschillen tussen de simulaties en de alternatieve testen.

Als eerste leiden de verschillen tussen de testopstellingen tot een aantal verschillen. Het blijkt dat het vergroten van de spoorstijfheid van het model door het aanpassen van de schaalfactor LKY zorgt voor een betere overeenkomst tussen het model en de metingen.

Ten tweede is het belangrijk om een goede basis van metingen te hebben. Het gebied waar geen metingen beschikbaar zijn, moet goed gecontroleerd worden!

Ten derde kwam in de dynamische testen de verticale kracht meestal goed overeen, alleen het maximum van de langs kracht was in alle gevallen te hoog. Dit is een bekend fenomeen van het MF-Tyre/MF-Swift model.

Als laatste was de frequentie van de simulaties te hoog. Het toevoegen van de dynamica van de test opstelling aan het simulatiemodel zal leiden tot een betere overeenkomst van de frequentie.

Notation

symbol	description
F_{x_C} (F_{x_H})	longitudinal force, expressed in axis system TYDEX C (H)
F_{y_C} (F_{y_H})	lateral force, expressed in axis system TYDEX C (H)
F_{z_C} (F_{z_H})	vertical force, expressed in axis system TYDEX C (H)
M_{x_C} (M_{x_H})	overturning moment, expressed in axis system TYDEX C (H)
M_{y_C} (M_{y_H})	rolling resistance moment, expressed in axis system TYDEX C (H)
M_{z_C} (M_{z_H})	self-aligning moment, expressed in axis system TYDEX C (H)
α	side slip angle
κ	longitudinal slip
γ	inclination angle
LMY	scale factor of rolling resistance torque
LKY	scale factor of cornering stiffness
LKX	scale factor of slip stiffness

Contents

Chapter 1

Introduction

Modern analysis of vehicle dynamic systems supports decisions of design and variants by means of simulation. Therefore reliable simulation models are needed, especially for the description of tyre behavior. As the part that connects the vehicle and the road, the tyre defines, for a great part, the vehicle dynamic behavior, usable safety reserves and the ride comfort caused by the road surface.

1.1 TMPT-Benchmark

To compare the performance of different tyre models, the TyreModel Performance Test-Benchmark (shortly TMPT) is established. Within that Benchmark several tyre model suppliers have agreed upon a set of measurements for the parameter determination of the tyre models. Professor Gipser with FTire, LMS with CD-Tire and TNO with MF-Tyre/MF-Swift have taken part at the Benchmark. The tyre model parameters were identified by the tyre model suppliers - here TNO-Automotive - and the tyre data set as well as the measured data is now available upon request.

The stationary tyre tests were carried out by Continental. The steady state lateral characteristics were measured following in principle the Time-protocol. At an inflation pressure of 2.0 and 2.5 bar the linear range (max. 1° slip angle) and the nonlinear range (max. 12° slip angle) were measured. Camber angle variations were done up to approx. 5.7°; the vertical load was variated up to approx. 9200 N.

The longitudinal behavior was measured with 2.0 bar under the vertical loads of 3000 N (≈50 % of LI[1]), 4700 N (≈80 % of LI), 6500 N (≈110 % of LI) and with 2.5 bar under the vertical loads of 1500 N, 2500 N, 3500 N and 6000 N. These longitudinal measurements should have been done up to ± 30 % of longitudinal slip, but for the higher vertical loads only longitudinal

[1] Load Index indicates the maximum load at a certain speed and inflation pressure

slip up to $\pm$ 3 % was applied. No combined measurements were done as well as no camber variations for the longitudinal load cases.

The dynamic tests were carried out by Michelin. Modal tests as well as 90°-cleat tests have been carried out. For the cleat tests 10*20 mm (height*length) and 20*20 mm cleats were used. The tyre pressure was varied within 2.0, 2.5 and 3.0 bar and the driving velocity between a speed lower than 5 km/h, 30 km/h and 60 km/h. The vertical displacement of the tyre was fixed corresponding to a vertical load of 50 % of LI, 80 % of LI and 110 % of LI. Not all those permutations were measured.

1.2 Testing MF-Tyre/MF-Swift

In order to get a better insight in the tyre behavior additional tests were done at the testrig in Karlsruhe ordered by DaimlerChrysler and MagnaSteyr. The tests were done with the tyre Continental 205/55 R16 90H (PCI-S) that is considered within the TMPT-Benchmark carried out by the University of Vienna (Professor Lugner). These tests were not used for the parameterization of the tyre model and therefore supply a good base to study the predictive behavior of the tyre model on those measurements.

The MF-Tyre/MF-Swift 6.0 tyre model is the latest development of TNO-Automotive. In this internship the MF-Tyre/MF-Swift tyre model is coupled to the multibody simulation system DADS. After that several tests are simulated on a virtual testrig implemented in DADS. These simulations will be compared with the additional measurements from Karlsruhe to study the predictive behavior of the tyre model. The parameter identification was done with MF-Tool 5.2 corresponding to MF-Tyre 5.2, whereas the tyre simulations were carried out with the latest version 6.0. Nevertheless the formulas are downward compatible.

1.3 Contents of this report

First, the coupling of MF-Tyre/MF-Swift 6.0 to DADS 9.60 is described in chapter two. Here it is explained what is done to make this tyre model work with this custom version of DADS.

Second, the testing of the predictive behavior of the MF-Tyre/MF-Swift tyre model is described in chapter three. In the first section the stationary behavior is studied and in the second section the dynamic behavior is tested. For every type of maneuver the results are shown and discussed. In the third section the effect of changing the cornering stiffness of the model is studied.

Finally the conclusions and recommendations are drawn in chapter four.

Chapter 2

Coupling MF-Tyre/MF-Swift to DADS

By extracting the file *MFTyre601_dads.tar*, three directories are made: bin, src and $test\_models$. In the bin directory, there are files which are needed to make the solver for DADS. In the src directory, there are some source files, which are needed to implement a user defined road. In the $test\_models$ directory, there are some DADS models which can be used to test the software.

2.1 Environments

The custom solver uses a shared library file called *tt-shared32.so*. To make sure the solver finds this file, the environment variable LD_LIBRARY_PATH must be set by using the setenv-command [3]. For example use the following command as a shell command: **setenv LD_LIBRARY_PATH .** (see figure 2.1). Now the solver searches in the working directory for the file *tt-shared32.so*, so make sure that this file is in the working directory. To check the defined shell variables, use the echo-command, e.g.: **echo $LD_LIBRARY_PATH** (see figure 2.1).

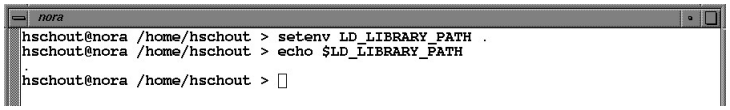

Figure 2.1: Setting and checking the LD_LIBRARY_PATH environment

The software also needs to find the license file. Therefore, the directory where the license file is located must be added to the environment LM_LICENSE_FILE [3]. To check the defined shell variables use the echo-command, e.g.: **echo $LM_LICENSE_FILE** (see figure 2.2). Here, the license file is located in the working directory, so this directory is added by using the

setenv-command, e.g.: **setenv LM_LICENSE_FILE ... :.** and replace the three dots with the directories which where already defined (see figure 2.2).

```
hschout@nora /home/hschout > echo $LM_LICENSE_FILE
27000@rtsutx9000:27000@wali:27000@widar:27002@rtsutx9015:27002@rtsutx9101:2700
rtsutx9102:27006@rtsutx9015:27006@rtsutx9101:27006@rtsutx9102:27003@rtsutx9000
7005@rtsutx9015:27005@rtsutx9101:27005@rtsutx9102:27007@rtsutx9015:27007@rtsut
101:27007@rtsutx9102:27008@rtsutx9015:27008@rtsutx9101:27008@rtsutx9102:/usr/l
al/flexlm/licenses/nora.nodelocked
hschout@nora /home/hschout > setenv LM_LICENSE_FILE 27000@rtsutx9000:27000@wal
27000@widar:27002@rtsutx9015:27002@rtsutx9101:27002@rtsutx9102:27006@rtsutx901
27006@rtsutx9101:27006@rtsutx9102:27003@rtsutx9000:27005@rtsutx9015:27005@rtsu
9101:27005@rtsutx9102:27007@rtsutx9015:27007@rtsutx9101:27007@rtsutx9102:27008
tsutx9015:27008@rtsutx9101:27008@rtsutx9102:/usr/local/flexlm/licenses/nora.no
locked:.
hschout@nora /home/hschout >
```

Figure 2.2: Setting the LM_LICENSE_PATH environment

By placing the commands, used to set both environments, in the *.login-file*, these environments are set every time you login. Here, it is placed in the *.tcshrc-file*, which runs every time you open a new shell, see figure 2.3. It is also possible to use a different location for the library file and the license file. In that case use the same commands, but replace the dot with the directory in which the file is located.

```
#-------------------------------------------------
# Adding two commands for using DelftTyre software.
# make the library path the working directory:
setenv LD_LIBRARY_PATH .

# add the working directory to the environment LM_LICENSE_FILE:
setenv LM_LICENSE_FILE 27000@rtsutx9000:27000@wali:27000@widar:27002@rtsutx9015:»
«27002@rtsutx9101:27002@rtsutx9102:27006@rtsutx9015:27006@rtsutx9101:27006@rtsutx»
«9102:27003@rtsutx9000:27005@rtsutx9015:27005@rtsutx9101:27005@rtsutx9102:27007@r»
«tsutx9015:27007@rtsutx9101:27007@rtsutx9102:27008@rtsutx9015:27008@rtsutx9101:27»
«008@rtsutx9102:/usr/local/flexlm/licenses/nora.nodelocked:.
#-------------------------------------------------
```

Figure 2.3: Part of the *.tcshrs-file*

2.2 Creating the solver

In figure 2.4 an overview of the structure of DADS is given. A model is created in the graphical user interface (GUI). After pre-processing the model it can be solved by the solver, which is the file *ndads3d.exe*. To implement a tyre model, a custom solver is needed. In the case of the MF-Tyre/MF-Swift model, this solver communicates with the tyre model using the standard tyre interface (STI). The tyre model communicates with the road description using the standard road interface (SRI).

Because DaimlerChrysler uses a custom version of DADS, the makefile which is normally used to create the solver, does not work. This makefile uses the command $make3$, but this command is not available. Therefore, we have to use the following makefile:

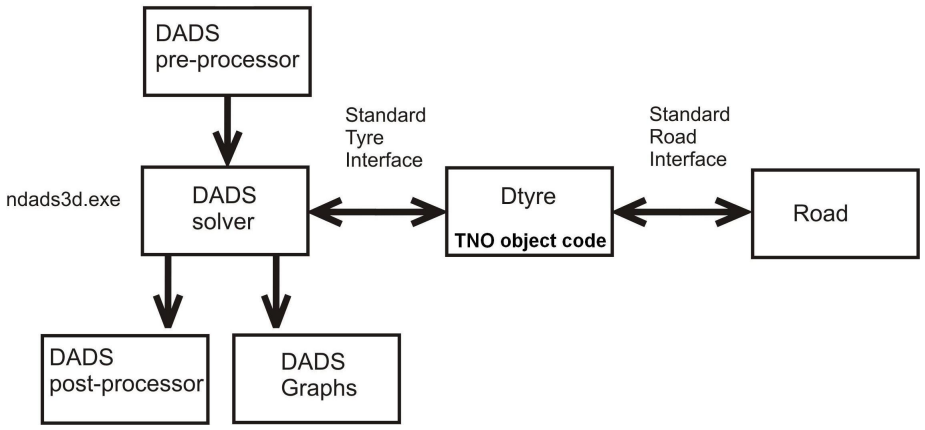

Figure 2.4: Overview of the structure of DADS

```
# Makefile for DADS with MF-Tyre/MF-Swift for DaimlerChrysler

.SUFFIXES: .o .f .bd

DADSLIBDIR =  /share/dads/dads96_217/sgi/dads96/dadslib/

DADSEXEDIR =  /share/dads/dads96_217/sgi/dads96/execute/

CASCADELIBDIR = /proj/CASCaDE/CAnew/IRIX_6_5_MIPS3/lib/

LMGRLIB =  liblmgr.a

CPPFLAGS = -c -v -g -n32

CTILIBDIR  = CTI_SGI_N32/

DADSLIBS= \
        ./patches/inter98.o \
        ./patches/analys.o \
        ./patches/frcudfj.o \
        ./patches/mm97.o \
        ./patches/ddastp.o \
        ./patches/step.o \
        ./patches/varlst.o \
        ./patches/preudf.o \
        ./patches/setbdfptr_sgi.o \
        ${DADSLIBDIR}blockda.o \
```

```
        ${DADSLIBDIR}revbd.o \
        ${DADSLIBDIR}xdummy.o \
        ${DADSLIBDIR}mod3d.a \
        ${DADSLIBDIR}analysis.a \
        ${DADSLIBDIR}super3d.a \
        ${DADSLIBDIR}mod3d.a \
        ${DADSLIBDIR}analysis.a \
        ${DADSLIBDIR}mod3d.a \
        ${DADSLIBDIR}controls3d.a \
        ${DADSLIBDIR}controls.a \
        ${DADSLIBDIR}harwell.a \
        ${DADSLIBDIR}tools.a \
        ${DADSLIBDIR}daftools.a \
        ${DADSLIBDIR}mathtools.a \
        ${DADSLIBDIR}dadsblas.a \
        ${DADSLIBDIR}${LMGRLIB} \
        ${DADSLIBDIR}libparent.a \
        ${DADSLIBDIR}libcp.a \
        ${DADSLIBDIR}ctools.a \
        ${DADSLIBDIR}expressionparser.a \
        ${DADSLIBDIR}mxxdummy.o \
        ${DADSLIBDIR}ortho.a \
        ${DADSLIBDIR}rte.a \
        ${DADSLIBDIR}flexread.a \
        ${DADSEXEDIR}durability/sgi6n3/lib/tmdmd_ld.o \
        ${DADSLIBDIR}cgdummy.o \
        ${DADSLIBDIR}ez5dummy.o \
        &{CASCADELIBDIR}libU.a
# libU.a is used for time measurement in dtyre.f

OBJS = \
    tno_protchk.o \
    tno_tyres_cat.o \
    tt_shared32.so \
    dtyre.o \
    dtemsg.o \
    tno_road2d.o \
    main.o

ndads3d : $(OBJS)
    f90 -u -g -n32 \
    -o ndads3d \
    ${DADSLIBDIR}progrm.o \
    ${DADSLIBDIR}matdummy.o \
```

```
    $(OBJS) \
    $(DADSLIBS) \
    /usr/lib32/c++init.o \
    -lC -lc

main.o : main.f
    f77 -c -u -g -n32 -mips3 main.f -o main.o
```

Replace the original makefile in the directory bin with the DaimlerChrysler-makefile and make sure that the file $main.f$ and the directory $patches$ are also in the bin directory. Before running the makefile, the original executable called $ndads3d$ has to be removed or renamed, otherwise the following notification will appear: 'UX:make: INFO: 'ndads3d' is up to date'. Now run the Daimler-Chrysler makefile by using the command **make** in the command shell. The final result will be a new executable called $ndads3d$, which is created in the same directory.

To make sure DADS uses this executable, copy this file to your working directory or set a symbolic link from the working directory to the $ndads3d$ executable. After a simulation, we can check if the right solver is used by viewing the inf-file. At the beginning of this file there must be a box of $TNOAutomotive$. There we can also see which version of Delft-Tyre software we are using, see figure 2.5.

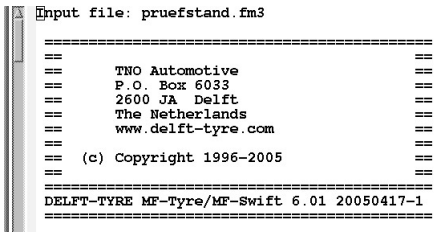

Figure 2.5: The inf-file with the TNO-box

2.3 GUI customization

2.3.1 Modify the STI Tyre menu

To take full advantage of the MF-Tyre/MF-Swift features we will need to modify the STI Tyre menu [3]. Then it is possible to adjust scaling factors directly in the DADS GUI. However, by changing the STI menu in DADS there will be problems when using other tyre-models. Therefore, the STI Tyre menu is not changed.

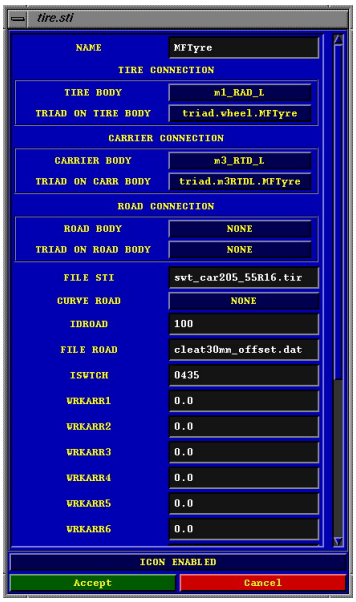

Figure 2.6: The original DADS STI Tyre menu

2.3.2 Signal names in DADSGraph

The signal names used by MF-Tyre/MF-Swift are different from the DADS default. It is possible to change the signal names in DADSGraph, but this can cause problems when using other tyre models. Therefore, the signal names are not changed. When using DADSGraph, the following translation table can be used [3]:

DADS	TNO / STI-convention
fx_chassis_body	longitudinal tyre force Fx
fy_chassis_body	lateral tyre force Fy
fz_chassis_body	vertical tyre force Fz
tx_chassis_body	overturning moment Mx
ty_chassis_body	rolling resistance moment My
tz_chassis_body	self-aligning moment Mz
fmg_chassis_body	force magnitude
tmg_chassis_body	moment magnitude
defl	longitudinal slip (kappa)
strs	side slip angle (alpha)
rlls	camber angle (gamma)
camb	turnslip
a	forward velocity Vx
fn	- not used -
flng	effective rolling radius
flat	vertical tyre deflection
fmag	contact length
fmax	pneumatic trail
almt	friction coeff longitudinal direction
frr	friction coeff lateral direction
fx_tire_body	relaxation length longitudinal
fy_tire_body	relaxation length lateral
fz_tire_body	Vsx
tx_tire_body	Vsy
ty_tire_body	vertical deflection velocity
tz_tire_body	- not used -
unx	kappa dynamic
uny	alpha dynamic
unz	- not used -
vn	travelled distance
vlng	- not used -
vlat	- not used -
tau	x coordinate contact point
v32	y coordinate contact point
v33	z coordinate contact point
v34	x road normal
v35	y road normal
v36	z road normal
v37	effective plane height
v38	effective plane angle
v39	effective plane curvature
v40	- not used -

Table 2.1: Translation table

Chapter 3

Testing MF-Tyre/MF-Swift

In this chapter the predictive behavior of the MF-Tyre/MF-Swift tyre model will be studied. First the stationary behavior and second the dynamic behavior will be tested. Finally a short study is done about the effect of changing the cornering stiffness.

3.1 Stationary tests

To check the stationary behavior of the tyre model three kinds of tests are done.

- First, pure cornering-tests are studied. In these tests the tyre is rolling over a flat road and a sweep of the side-slip angle is applied.
- Second, pure braking-tests are done. In this test the tyre is rolling over a flat road with varying longitudinal slip.
- Finally, combined slip-tests are considered, where the tyre is rolling over a flat road with a constant side slip angle and a varying longitudinal slip.

All stationary test are done with two different wheel loads of 3000 N and 6600 N.

3.1.1 Measurements

The measurements were done at the university of Karlsruhe on an internal drum test rig with a diameter of 3,8 m [2]. In table 3.1 more detailed information about the measurements is given.

The stationary tests are done with a forward velocity of 40 km/h. During the tests the wheel load F_z is controlled and the inclination angle γ is kept constant. In case of the pure cornering-test only the side slip angle α is varied. In case of the pure braking-test and the combined slip-test only the longitudinal slip κ is varied. A correction of the influence of the drum curvature is done by the university of Karlsuhe.

Measurement ID	TMPT-benchmark
Test rig	IPS
Tyre	205/55 R16 90 H
Manufacturer	Continental
Inflation pressure	2,5 Bar
Rim	6,5 J x 16
Road surface	Asphalt
Road condition	dry
Grain size	0/16
Roughness depth	$R_t = 0.84$ mm $\pm$ 0.1 mm
Grip	SRT $= 65 \pm 2$
Surrounding temperature	20° C - 25° C

Table 3.1: Details about the test rig

The format of the measured data is conform to the TYDEX-standard. The measurements are given within the TYDEX-H-axis system, see figure 3.1. However, the wheel load is controlled using TYDEX-C-axis system, see figure 3.2. The difference between these two axis systems is that the C-axis system is inclined. Therefore, there is a deviation between the wheel load in the H-axis system F_{z_H} and the wheel load in the C-axis system F_{z_C} if the tyre has an inclination angle.

3.1.2 Simulations

To simulate these tests within DADS, a virtual test rig is used in which a tyre and a carrier body are modeled. Using the parameter ISWTCH the operating mode of the MF-Tyre/Swift tyre model can be set in the STI GUI menu. For this test ISWTCH is chosen to be 2005.

- The first digit determines on which side the tyre is. The assumption that the tyre was an the right side during the tests gave the best coincidence with the measurements.
- The second digit determines the road contact method. Because the tyre runs over a flat road, the single contact point method is used.
- With the third digit the rigid ring dynamics are set. By using the value zero, the rigid ring dynamics are turned off. In this way only the stationary forces and moments are calculated. By switching off the dynamics and using a single contact point, the simulation speed is very high.
- The last digit determines the force evaluation. By using the value five the combined forces and moments are evaluated and turnslip is included.

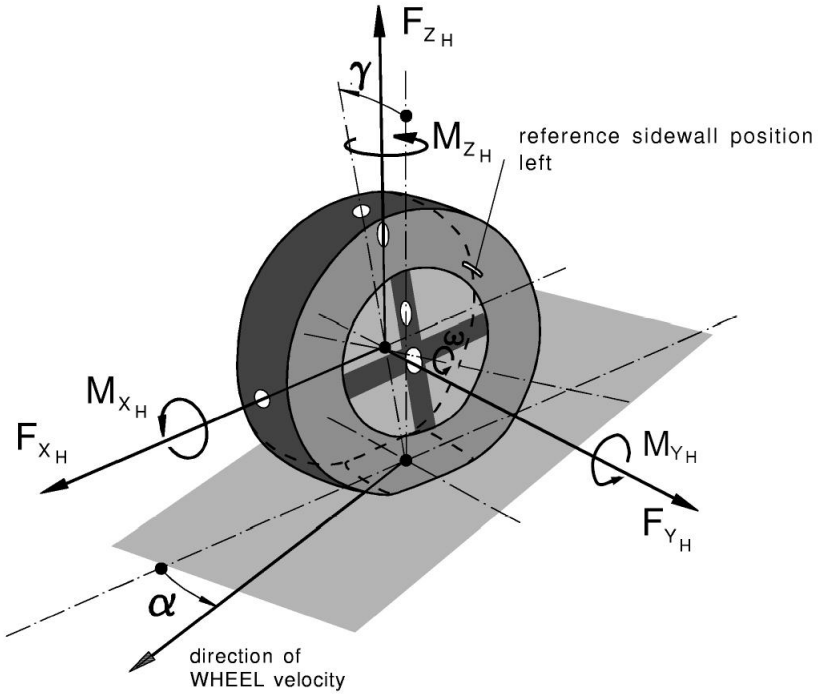

Figure 3.1: TYDEX-H-axis system

For more information about the operating modes of the tyre model, see the TNO tutorial [4].

The forces and moments are extracted from the simulation in the revolute joint between the hub and the wheel, on the triad used for the MF-Tyre/MF-Swift model, see figure 3.3. This axis system is equal to the TYDEX-C-axis system, so the forces and moments have to be transformed to the TYDEX-H-axis system with the following relations:

$$F_{y_H} = F_{y_C} \cos\gamma - F_{z_C} \sin\gamma \tag{3.1}$$

$$M_{y_H} = M_{y_C} \cos\gamma - M_{z_C} \sin\gamma \tag{3.2}$$

$$F_{z_H} = F_{z_C} \cos\gamma + F_{y_C} \sin\gamma \tag{3.3}$$

$$M_{z_H} = M_{z_C} \cos\gamma + M_{y_C} \sin\gamma \tag{3.4}$$

Note that for very small inclination angles, the difference between the two axis-systems is negligible. Because later on simulations will be made with bigger inclination angles, these transformations are used.

Within the simulation the invariant parameters are adjusted to match those of the measurements.

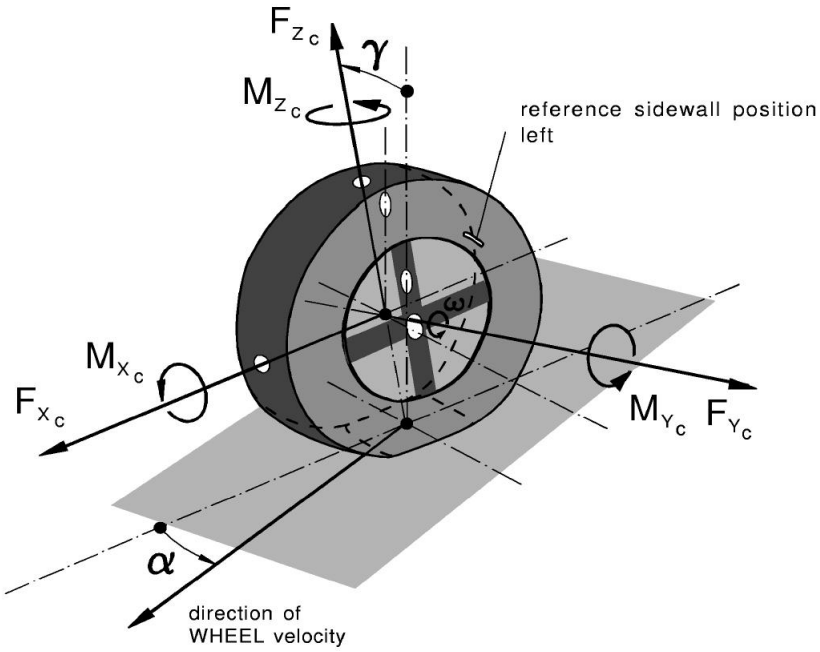

Figure 3.2: TYDEX-C-axis system

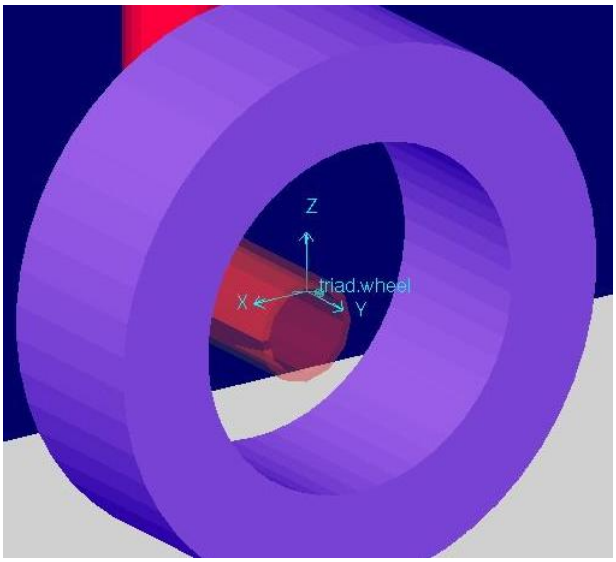

Figure 3.3: Test rig in DADS showing the triad used for MF-Tyre/MF-Swift

3.1.3 Results

In this section the results of the stationary simulations will be compared to the measurements. For every test the most important figures are shown, see appendix A, B and C for more plots. For each type of maneuver you will find the discussion after the diagrams. In the stationary tests all forces and moments are expressed in the H-axis system.

Pure cornering with a load of 3000 N

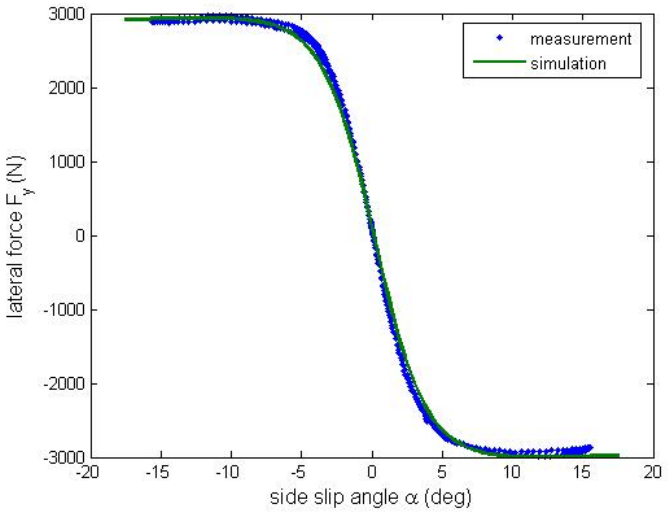

Figure 3.4: Lateral force F_{y_H} (N)

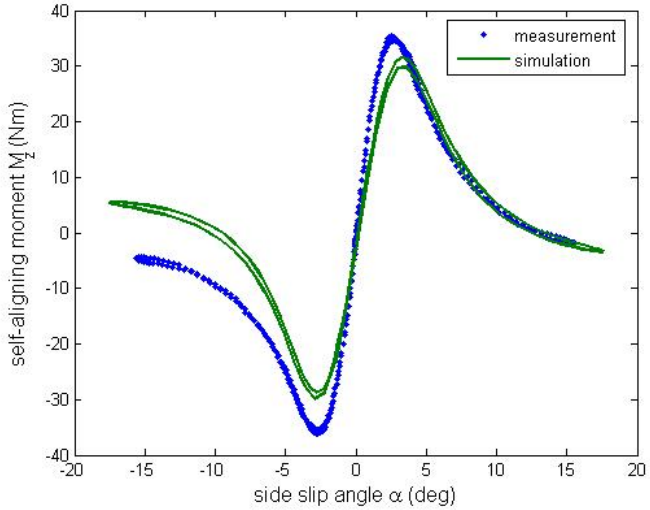

Figure 3.5: Self-aligning moment M_{z_H} (Nm)

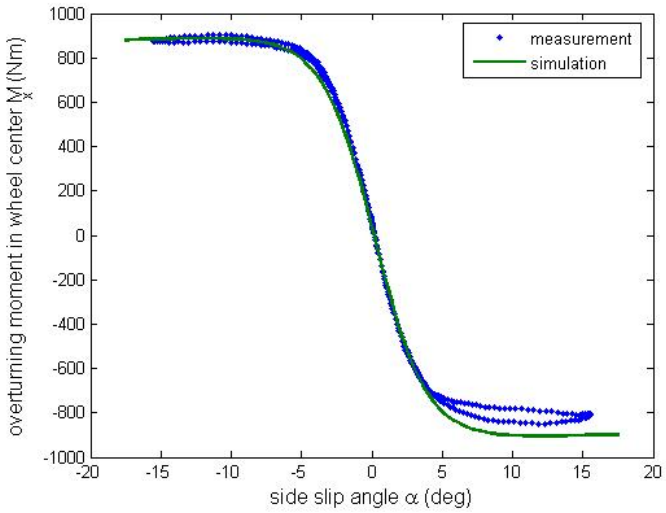

Figure 3.6: Overturning moment in wheel center M_{x_H} (Nm)

Pure cornering with a load of 6600 N

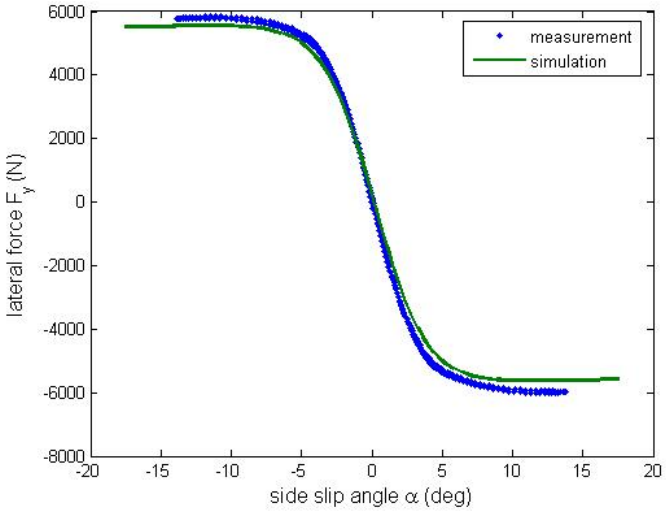

Figure 3.7: Lateral force F_{y_H} (N)

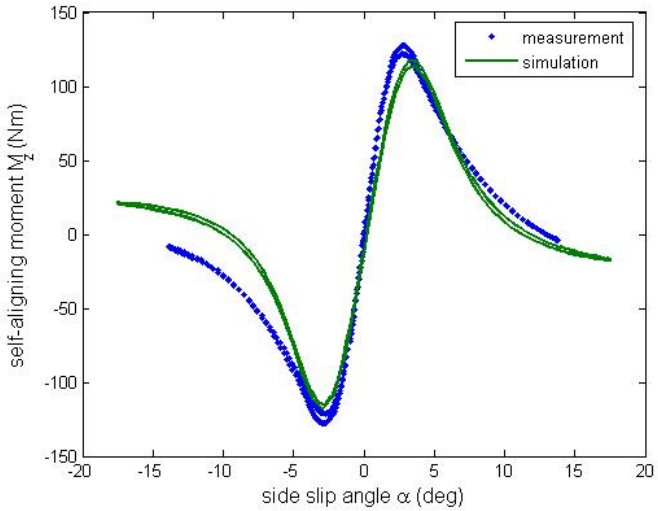

Figure 3.8: Self-aligning moment M_{z_H} (Nm)

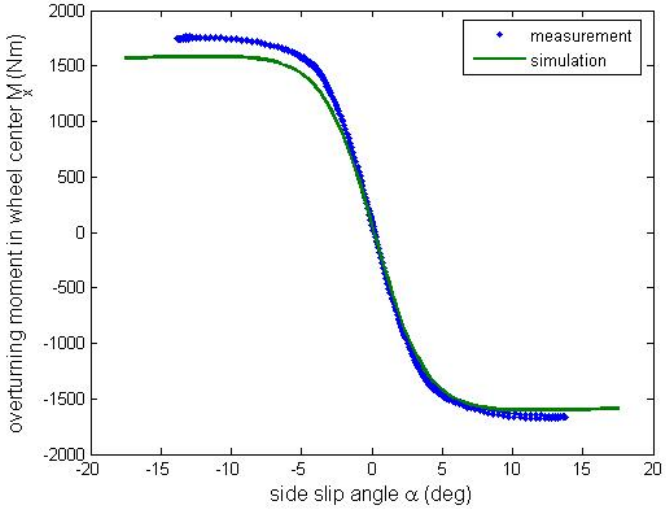

Figure 3.9: Overturning moment in wheel center M_{x_H} (Nm)

Conclusions regarding the pure cornering-tests

From figure 3.4 it can be seen that the maximum side force of the simulation matches well with the measurement when a vertical load of 3000 N is applied. But in case of a vertical load of 6600 N the maximum side force is too low as can be seen in figure 3.7. In both tests the cornering stiffness of the model is also too low. The difference between the cornering stiffness of the model and the measurements is for a wheel load of 3000 N about 15 % and for a wheel load of 6600 N about 13 %.

These differences can be explained by the differences in the test rigs. The original TMPT-measurements were done on an external drum with a diameter of 2 m. No curvature correction was done upon the measurements. Because of the curvature, the contact length is smaller than on a flat road or the inner drum test rig, which results in smaller side forces. The tyre model parameters are identified using the measurements on the external drum. The compared measurements were done on an internal drum. A curvature correction was carried out on those measurements. The resulting difference in the contact patch will result in a different cornering stiffness and maximum value. Also the vertical force decreases for bigger side slip angles, this also has an impact on the side forces.

The cornering stiffness can be adapted by changing the scaling factor LKY in the tyre property file[1], this is done in chapter 3.3.

The surface property has also an impact on the maximum value of the side force, but less impact on the cornering stiffness. The original measurements

[1] how the parameter set of the MF-Tyre/Swift is named

were done on Safety Walk, whereas the measurements for the comparison were done on asphalt. With the friction-scaling factor the maximum of the side force may also be changed.

In figure 3.5 and 3.8 is again visible that the stiffnesses are too low. This is also a result of the difference in contact length. When adjusting the cornering stiffness this will also improve the stiffness of the self-aligning moment.

A second effect which plays a role here is crosstalk. In the compared measurements there is a crosstalk up to 0.5 % between the overturning moment M_{x_H} and the self-aligning moment M_{z_H} to be expected [2]. An overturning moment of 900 Nm implies a difference of 4,5 N. The deviation of the self-aligning moment M_{z_H} ranges within this inaccuracy of the measurement system.

Although the maximum of the corresponding side force matches the measurement, the maximum overturning moment M_{x_H} in figure 3.6 shows a deviation with the measurements. This may be a result of crosstalk. The overturning moment should be mainly the side force times tyre radius, what can be seen in 3.9. For the 3000 N vertical load case in picture 3.6 the deviation for positive side slip angles is unexpected; the measurements show an asymmetric behavior that is not to be seen at the 6600 N load case. This cannot be derived from the decrease of the vertical load since this has minor impact on the side force here.

The longitudinal forces F_{x_H} in figure A.1 and figure A.4 don't match well with the measurements. Because there were no measurements of the rolling resistance done for the parameterization of the tyre model, a default value for the rolling resistance is used. This rolling resistance can be changed using the scalingfactor LMY, whereby longitudinal force characteristic of the model improves a lot. Note that this scaling factor only effects the rolling resistance, so changing it does not change other properties of the tyre.

It can be seen in picture A.4 that in the measurements the longitudinal force F_{x_H} becomes positive, which is very unlikely. This can be a result of crosstalk between the sideforce and the longitudinal force, which may be up to 0.5 % [2]. With a sideforce of 6600 N, this results in a longitudinal force of 33 N.

Throughout the measurements the vertical load is varying although controlled to be constant. When applying a side sweep the radius of the tyre changes what results in a difficulty to keep the vertical load constant.

Pure longitudinal slip with a load of 3000 N

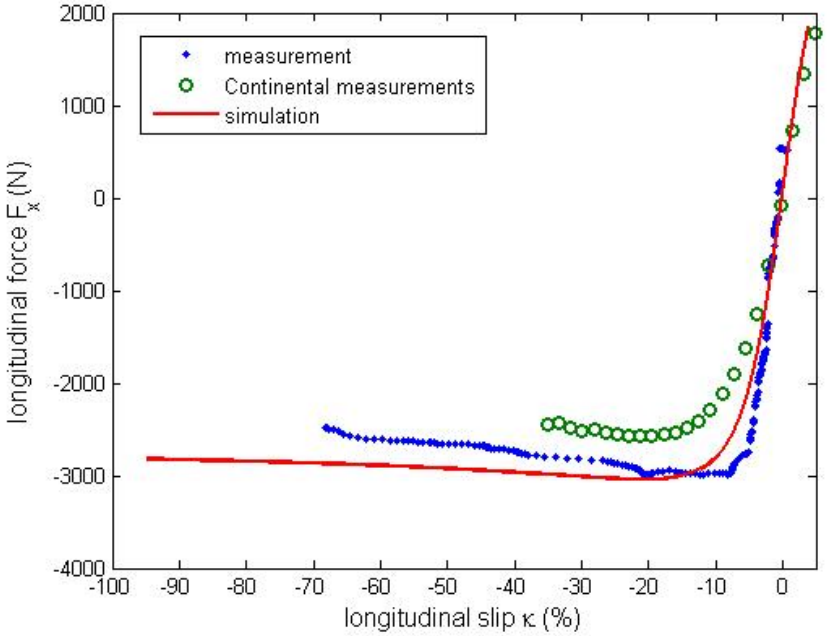

Figure 3.10: Longitudinal force F_{x_H} (N), note that the Continental measurements are done with a wheel load of 2500 N

Pure longitudinal slip with a load of 6600 N

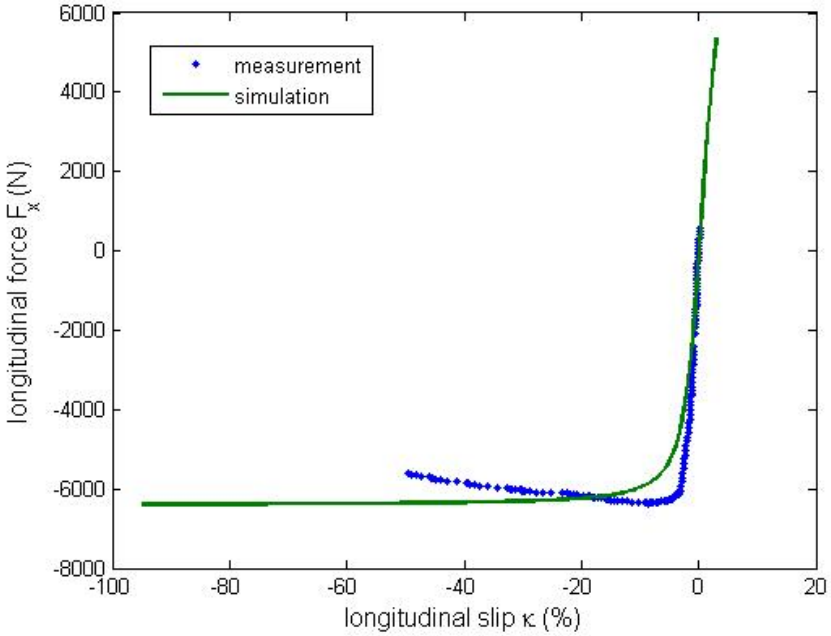

Figure 3.11: Longitudinal force F_{x_H} (N)

Conclusions regarding the pure longitudinal slip-tests

We can divide figure 3.10 and 3.11 into three parts. The first part is from 0 to approx. -5 % longitudinal slip, the stiffness-part. In this part it can be seen that the stiffness of the model is too low compared to the measurements. This is a result of the difference in contact length due to the different curvature in the measurements as already mentioned. In this part the vertical force is higher for the measurements, which also results in an increased stiffness. This stiffness can be changed with the scaling factor LKX, but this is not done here.

The second part is approximately between -5 to -20 % longitudinal slip. In this part the simulations and the measurements don't match well. The long linear characteristic followed by an abrupt change in the measurements is not very common. Also the Continental measurements used for parameterization do not show this behavior, see figure 3.10. The behavior is usually expected to be more smooth. Very important in this test is, how to apply a brake torque to the tyre. When doing this too fast, the dynamics of the tyre become important, so the tyre is not in steady-state mode anymore. When doing it too slow, the temperature of the tyre will increase, which will also affect the tyre behavior.

The third part is from approx. -20 to -100 % longitudinal slip. Here the vertical force of the measurements is much lower, which results in a lower longitudinal force F_{x_H}. However, with a load of 3000 N the decrease of longitudinal force of the tyre model is very small and with a load of 6600 N there is no decrease at all. This is not very usual for MF-Tyre/MF-Swift. The reason for this is that there were no measurements available with a load of 6600 N and more than 3 % longitudinal slip, when parameterizing the tyre model. With smaller vertical loads there were only measurements up to 30% slip done by Continental. Within that final part the measurements show a more reasonable behavior than the tyre model due to an unrealistic extrapolation of the tyre model. The behavior of the tyre model can be improved by fixing more parameters during the fitting process, which is not done in the parameterization so far.

Because the side slip angle α is about zero, the lateral force F_{y_H}, the self-aligning moment M_{z_H} and the overturning moment M_{x_H} are very small. Therefore the differences look very big and the measurements have a lot of noise. The self-aligning moment M_{z_H} under braking is always difficult to predict. The vertical load changes a lot while braking.

Combined slip with a load of 3000 N

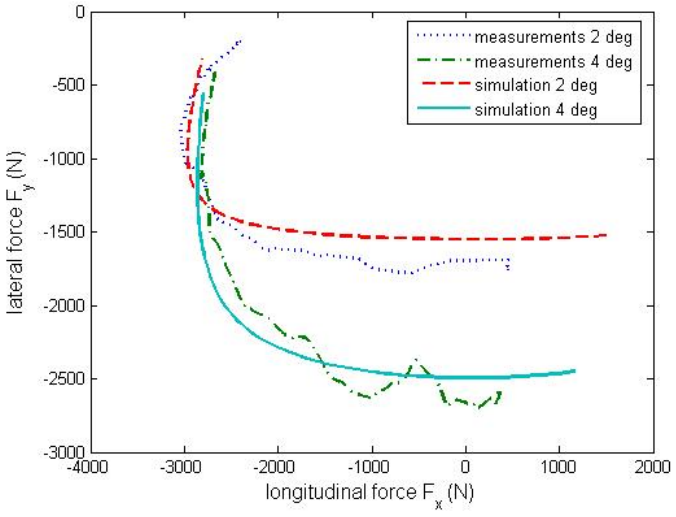

Figure 3.12: Lateral force F_{y_H} as a function of longitudinal force F_{x_H}

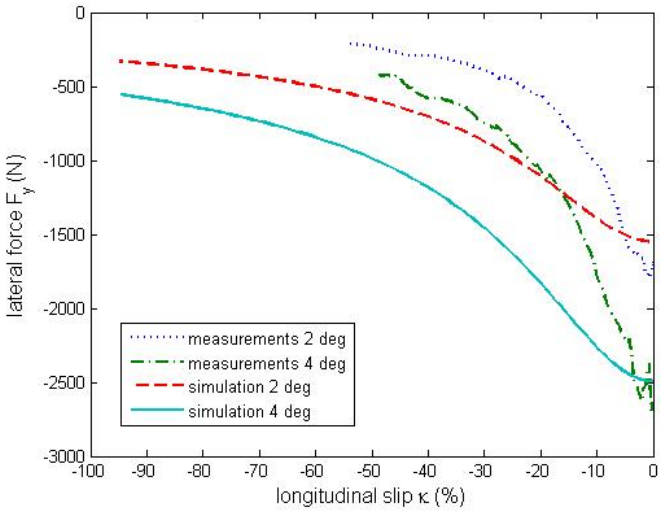

Figure 3.13: Lateral force F_{y_H}

Combined slip with a load of 6600 N

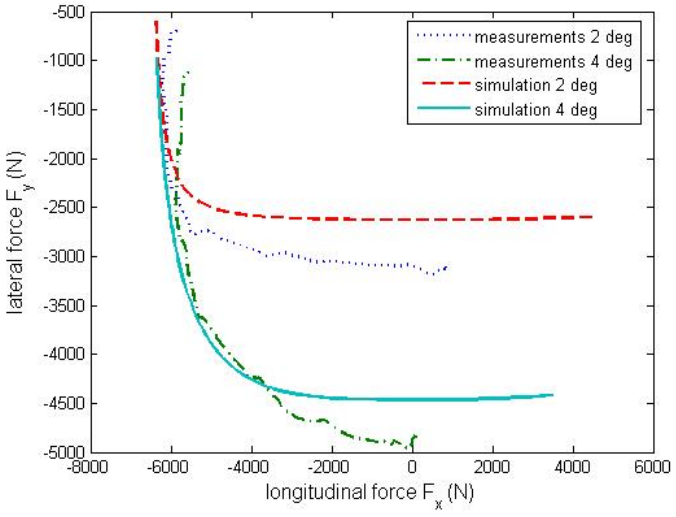

Figure 3.14: Lateral force F_{y_H} as a function of longitudinal force F_{x_H}

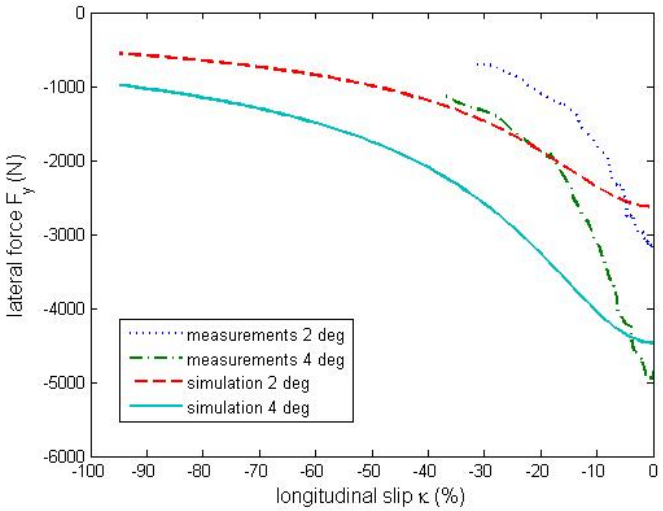

Figure 3.15: Lateral force F_{y_H}

Conclusions regarding the combined slip-tests

The combined characteristic in figure 3.12 and 3.14 matches quite well with the measurements. However, in figure 3.13 and 3.15, the lateral force matches not so well. Because there were no measurements with a high load and more than 3 % longitudinal slip available for the parameterization, as well as no combined measurements, the model matches not so good for higher longitudinal slip with a high load. The base of measurements for the parameterization was very incomplete for the longitudinal load cases. The extrapolation of the model is also not well, since the side force for 100% longitudinal slip should be closer to zero. This can be improved by fixing more parameters during the fitting process, which is not done so far.

As a result of this, the overturning moment M_{x_H} matches also not so well. Increasing the cornering stiffness of the model as already discussed beforehand will result in bigger sideforces and therefore in a better match with the measurements. This will be discussed in section 3.3.

3.2 Dynamic tests

In order to check the dynamic behavior of the model several cleat-tests are simulated and compared with the measurements [2]. The tests and the measurements have been carried out with a fixed distance of the wheel center with respect to the road surface. Two different wheel center heights are used, which correspond to a wheel load of 1700 N and 4800 N, when rolling over the flat surface.

3.2.1 Measurements

In the first two tests the tyre runs over a transversal 30*80 mm cleat with a forward velocity of 2 km/h. See figure 3.16 for more details about the cleat and see table 3.1 for more details about the test rig [2]. The slow velocity had to be chosen within this test, since the testrig, that is capable to measure up to 15 kN of vertical load, has a sample rate of 100 Hz. Vertical loads up to 8 kN can be measured at the testrig in Karlsruhe with a sample rate of 10 kHz, but with those large cleats the vertical loads exceed far that limit. Since the vehicle tests on the rough roads are done with speeds of 30 up to 60 km/h this circumstance is unsatisfying. The tyre shows a completely different characteristic at low speed then on those higher speeds due to the enveloping effect.

In the other tests a 10*28 mm cleat is used, see figure 3.17. These tests are done with a forward velocity of 2 km/h and 30 km/h. Since the vertical loads that occur during this test are under 8 kN the dynamic measurement hub could be used with a sample rate of 10 kHz. The small cleat may not resemble very well the obstacles on rough roads, but since the vertical distance of the hub is fixed the 10*28 mm cleat has more impact on the tyre within the testrig than when passing it on the real street. For the dynamic measurements the TYDEX-C-axis system is used, see figure 3.2.

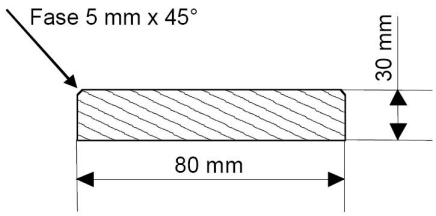

Figure 3.16: Sideview of the 30 mm cleat

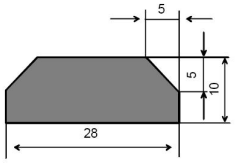

Figure 3.17: Sideview of the 10 mm cleat

3.2.2 Simulations

To simulate this cleat tests within DADS the wheel center height must be chosen in a way that the right wheel load F_{z_C} is achieved when rolling over the flat surface. To describe the road the TNO road description is used. In this 2D road description, the road height z is given for every road position x, with a linear interpolation between the given points. There are two columns with z-values; the first column is for the left track and the second column is for the right track. In this case both tracks are the same. The following file is the description of the 10*28 mm cleat:

```
$-------------------------------------------------------------MDI_HEADER
[MDI_HEADER]
FILE_TYPE  =  'rdf'
FILE_VERSION  =  5.00
FILE_FORMAT  =  'ASCII'
(COMMENTS)
{comment_string}
'polyline style road description'
$----------------------------------------------------------------------UNITS
[UNITS]
 MASS               = 'kg'
 LENGTH             = 'meter'
 TIME               = 'sec'
 ANGLE              = 'degree'
 FORCE              = 'newton'
$---------------------------------------------------------------------MODEL
[MODEL]

 METHOD             = '2D'
 ROAD_TYPE          = 'poly_line'
$-----------------------------------------------------------PARAMETERS
[PARAMETERS]
 OFFSET                  =   0
```

```
 ROTATION_ANGLE_XY_PLANE =   0
 MU                      =   1
$
(XZ_DATA)
    -10         0         0
      4.99999   0         0
      5.000     0.005     0.005
      5.005     0.010     0.010
      5.023     0.010     0.010
      5.028     0.005     0.005
      5.02801   0         0
     10         0         0
```

The used value for the parameter ISWTCH is 2435.

- Consistent to the stationary studies we assume that the tyre is on the right side during the measurements, so we also simulate with a tyre on the right side.
- With the second digit a 2D road contact method is selected (enveloping behavior). This contact method uses basic functions to evaluate the road.
- With the third digit the rigid ring dynamics are switched on in order to be able to calculate the dynamic behavior of the tyre up to 60 Hz.
- The last digit determines the force evaluation. By using the value five the combined forces and moments are evaluated and turnslip is included.

See the TNO tutorial [4] for more information about the operating modes of the tyre model.

The forces and moments are extracted from the simulation in the same triad as used for the cornering test, see figure 3.3. Within the simulations the forward velocity and the inclination angle are adjusted to match those of the measurements.

3.2.3 Results

In this section the results of the dynamic simulations and the measurements will be shown and for every test conclusions will be drawn. For every test a plot of the vertical force and the longitudinal force will be shown. See appendix D, E and F for plots of the lateral force, the overturning moment, the self-aligning moment, the inclination angle and the side slip angle. In the dynamic tests all forces and moments are expressed in the C-axis system.

30 mm cleat, wheel center height resulting in a load of 1700 N

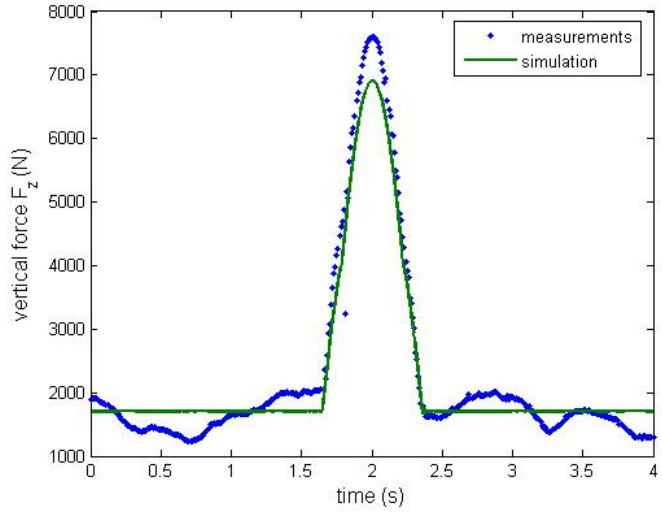

Figure 3.18: Vertical force F_{z_C} (N)

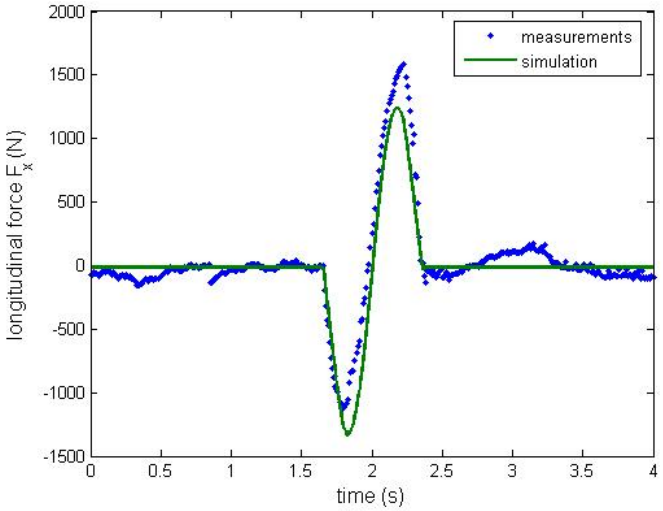

Figure 3.19: Longitudinal force F_{x_C} (N)

30 mm cleat, wheel center height resulting in a load of 4800 N

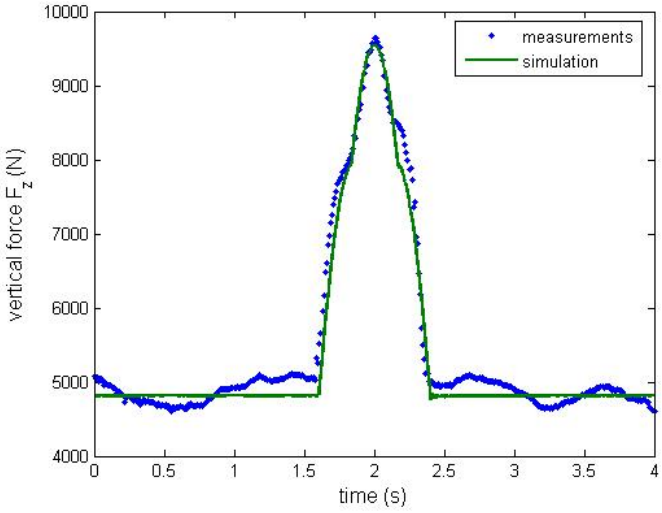

Figure 3.20: Vertical force F_{z_C} (N)

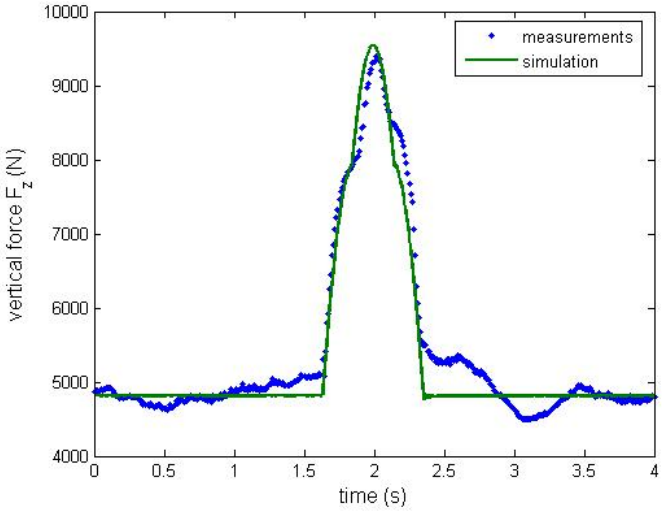

Figure 3.21: Vertical force F_{z_C} (N), second run

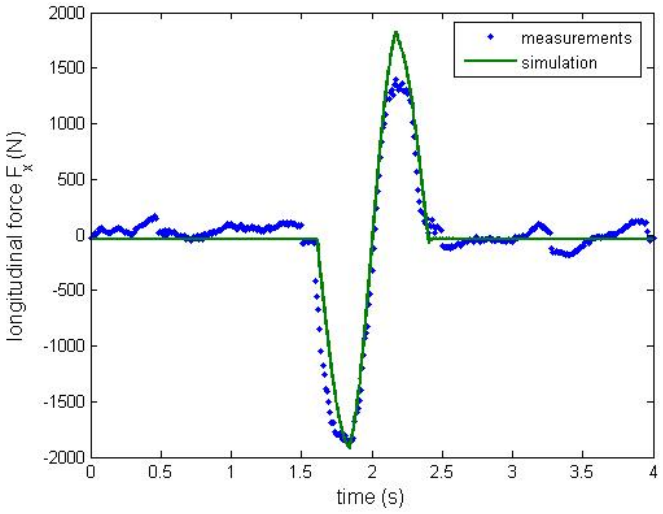

Figure 3.22: Longitudinal force F_{x_C} (N)

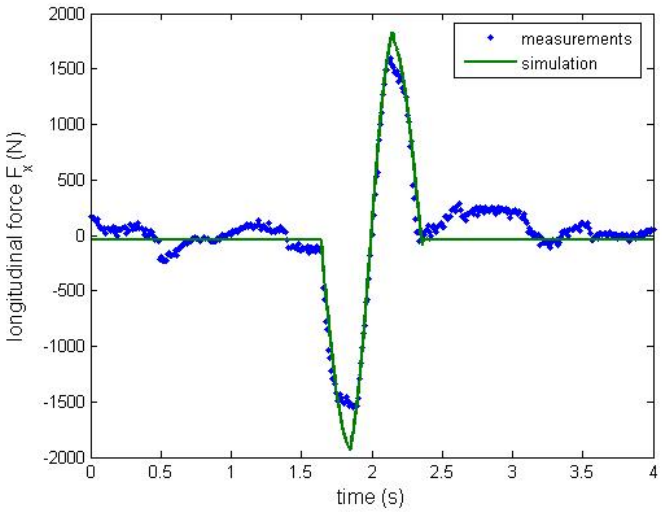

Figure 3.23: Longitudinal force F_{x_C} (N), second run

Conclusions of the 30 mm cleat-tests

During these tests the inclination angle γ and the side slip angle α are constant. However, as a result of internal vibration of the rigid ring and the contact patch, a very small reaction of the contact patch occurs. The extracted side slip value is the internal state of the tyre kinematic side slip angle seen by the contact patch.

The variation in the vertical force F_{z_C} in the measurements before and after rolling over the cleat, is a result of the variation of the surface of the test rig. When taken this variation into account, the vertical force of the simulations matches very good with the measurements.

In figure 3.19 and 3.22, it can be seen that the reaction of the longitudinal force F_{x_C} of the measurements are not symmetric. The model however shows a symmetric behavior, which is expected to be more realistic. This symmetric behavior is also visible in the second run of the last measured test, see figure 3.23.

The maximum values of the simulated longitudinal force F_{x_C} are too big in both tests. This could be adjusted by scaling the slope factor down, but that was not done here. The phenomenon that the simulated longitudinal forces are predicted too big is known; scaling strategies are supposed, but not undertaken here.

The lateral forces F_{y_C} are very small and the simulated values are within the noise level of the measurements.

The measured step-reaction in the overturning moment M_{x_C} is curious and may be a result of the unsymmetrical test rig. In the test rig of Karslruhe the axle is only fixed at one side, so perhaps the test setup is not stiff enough.

10 mm cleat with 2 km/h, wheel center height resulting in a load of 3000 N

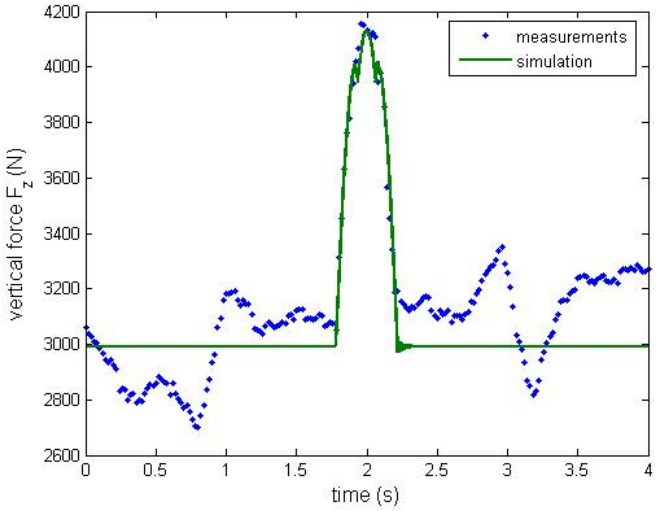

Figure 3.24: Vertical force F_{z_C} (N)

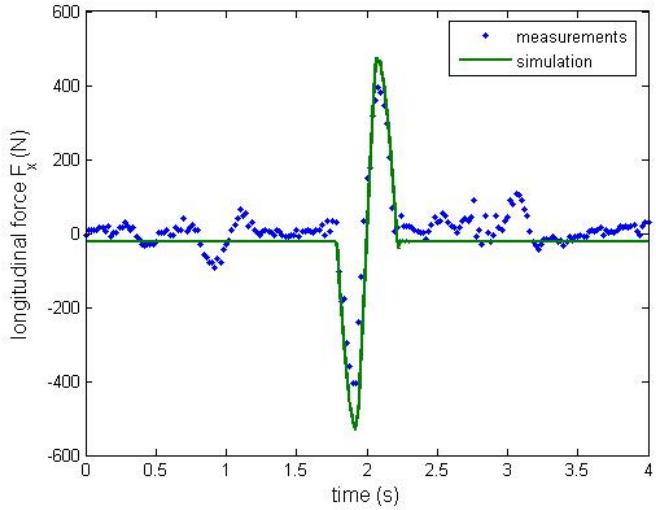

Figure 3.25: Longitudinal force F_{x_C} (N)

10 mm cleat with 2 km/h, wheel center height resulting in a load of 4800 N

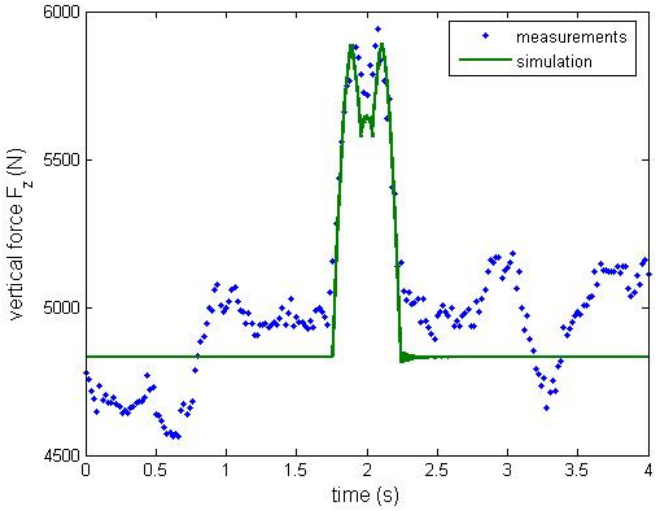

Figure 3.26: Vertical force F_{z_C} (N)

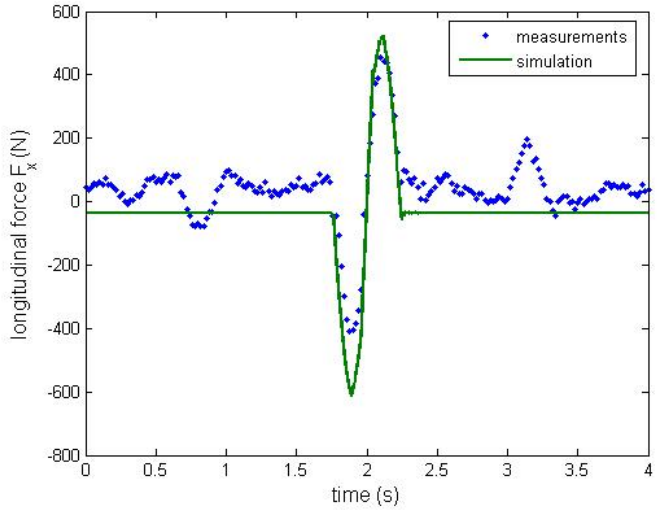

Figure 3.27: Longitudinal force F_{x_C} (N)

Conclusions of the 10 mm cleat-tests with 2 km/h

The vertical force F_{z_C} matches very well with the measurements. However, in the second test, see figure 3.26, the vertical force decreases a bit too much. Again the maximum values of the longitudinal force F_{x_C} are too high in both tests. The measurements of the lateral forces F_{y_C}, the self-aligning moments M_{z_C} and the overturning moments M_{x_C} are very small and very noisy.

10 mm cleat with 30 km/h, wheel center height resulting in a load of 3000 N

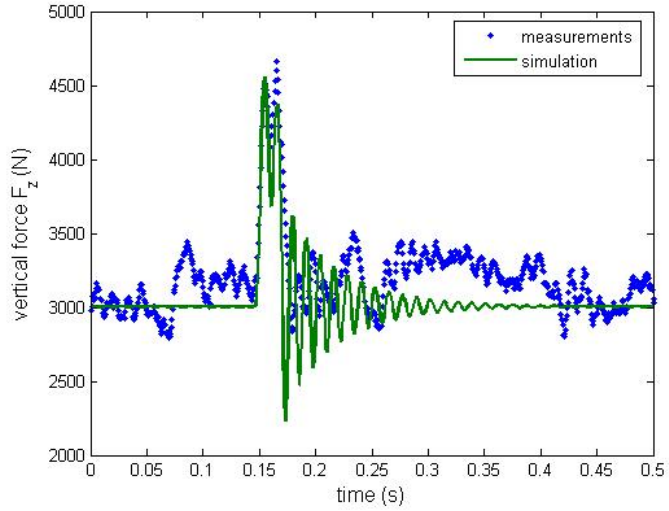

Figure 3.28: Vertical force F_{z_C} (N)

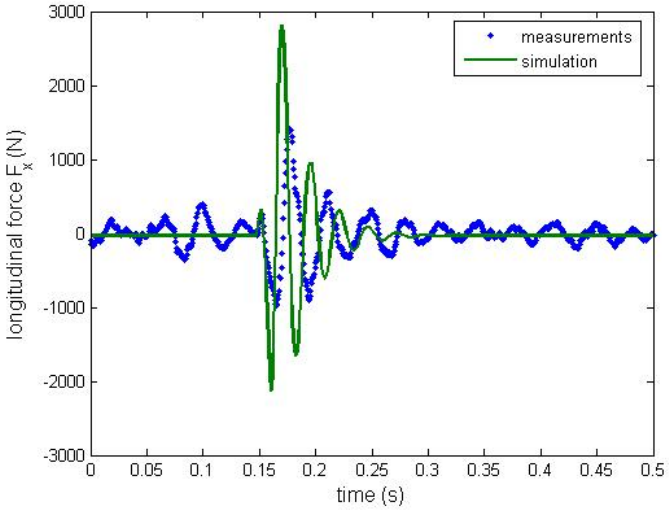

Figure 3.29: Longitudinal force F_{x_C} (N)

10 mm cleat with 30 km/h, wheel center height resulting in a load of 4800 N

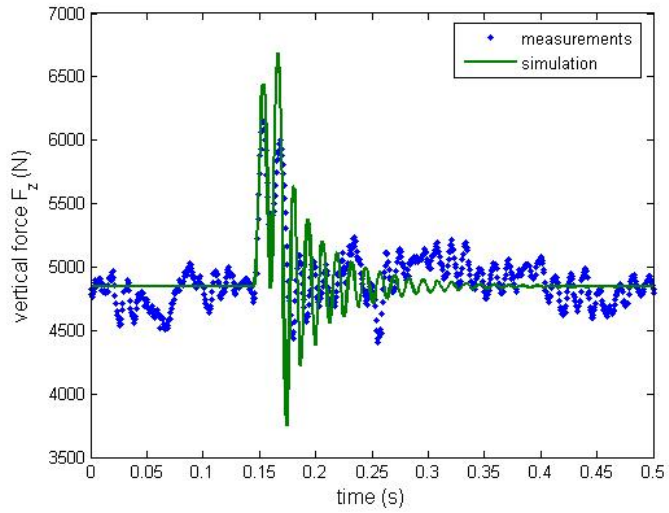

Figure 3.30: Vertical force F_{z_C} (N)

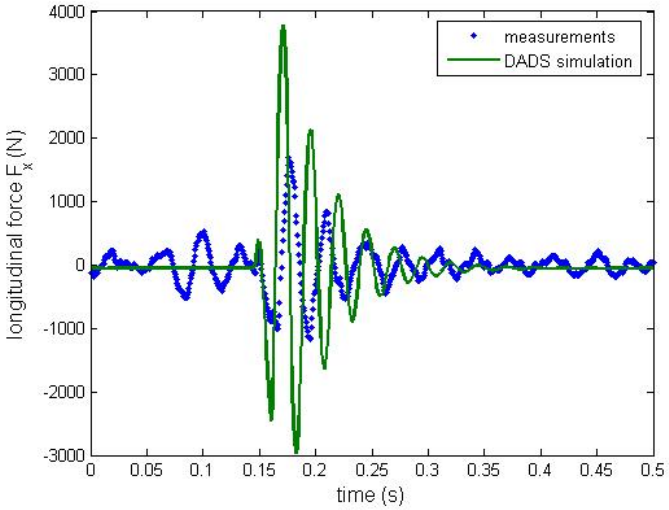

Figure 3.31: Longitudinal force F_{x_C} (N)

Conclusions of the 10 mm cleat-tests with 30 km/h

The vertical force F_{z_C} matches not so well with the measurements, also when taken into account the variations in the road surface of the test rig. The Peak-To-Peak-Distance is fairly different.

Also the frequency matches not well with the measurements. This can be a result of the stiffness of the test rig. With this high forces and high speeds the dynamics of the test rig become important. In the simulations within DADS the dynamics of the test rig are not taken into account; the test rig is infinite stiff. Therefore the frequency of the simulation is higher.

The longitudinal force F_{x_C} is much too high and the frequency is also too high.

The measurements of the lateral forces F_{y_C}, the self-aligning moments M_{z_C} and the overturning moments M_{x_C} are very small and very noisy.

The parameters for the enveloping behavior should be changed. The enveloping behavior is the geometric consideration when crossing the road surface (basic functions) what is completely separated from the tyre behavior due to the behavior of the belt [1]. By adjusting the enveloping behavior the slopes are tuned that the tyre sees when driving over the obstacles. It is clear that this has a direct impact on the longitudinal force reaction.

3.3 Changing the cornering stiffness

In the stationary tests of section 3.1.3 it is shown that the cornering stiffness of the model is too low (13 - 15 %). The cornering stiffness can be adapted by changing the scaling factor LKY in the tyre property file, but that was not done there. In this section the effect of changing LKY is studied. Therefore, the cornering stiffness is increased with 13 % and a pure cornering-test and a combined slip-test with 2 degrees of side slip are simulated, both with a wheel load of 3000 N.

3.3.1 Results of the pure cornering-test

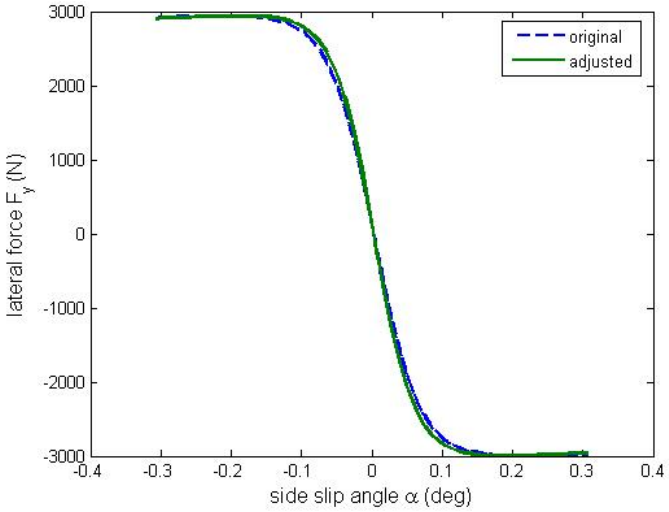

Figure 3.32: Lateral force F_{y_H} (N)

In figure 3.32 it can be seen that changing LKY only affects the cornering stiffness and not the maximum value of the lateral force F_{y_H}. As a result of the increased cornering stiffness, the stiffnesses of the self-aligning moment M_{z_H} (figure 3.33) and of the overturning moment M_{x_H} (figure 3.34) also increases.

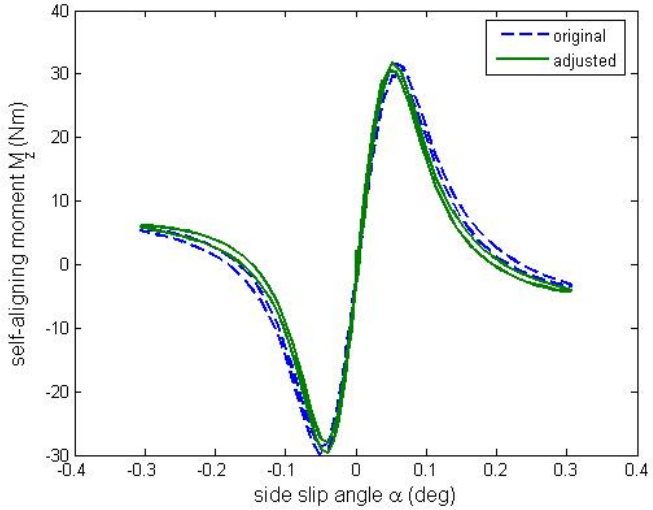

Figure 3.33: Self-aligning moment M_{z_H} (Nm)

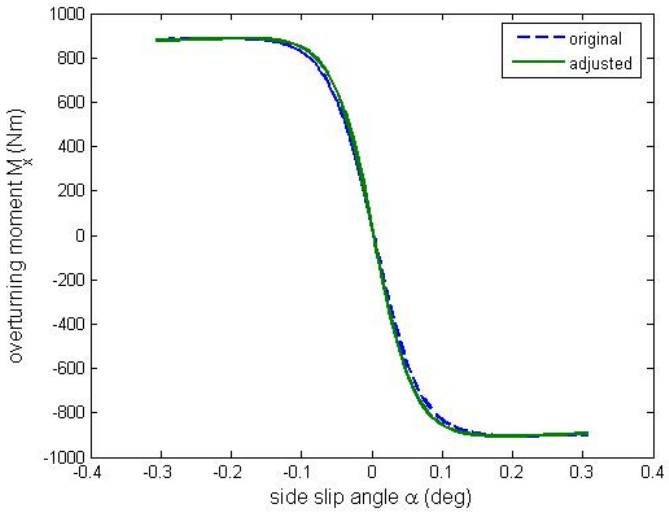

Figure 3.34: Overturning moment M_{x_H} (Nm)

3.3.2 Results of the combined slip-test

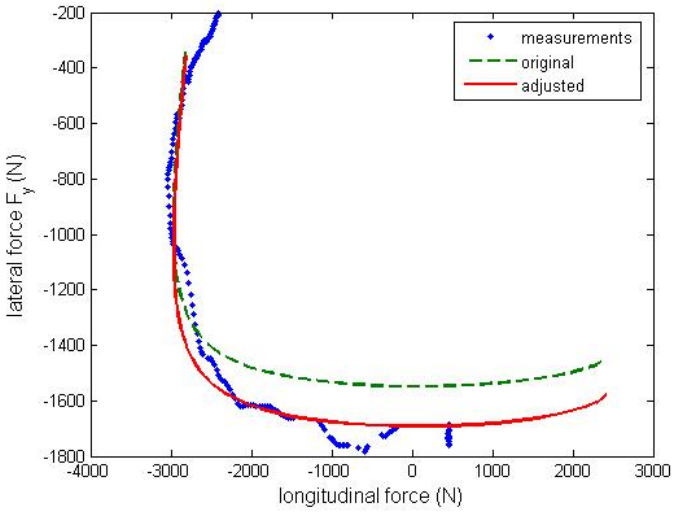

Figure 3.35: Lateral force F_{y_H} as a function of longitudinal force F_{x_H}

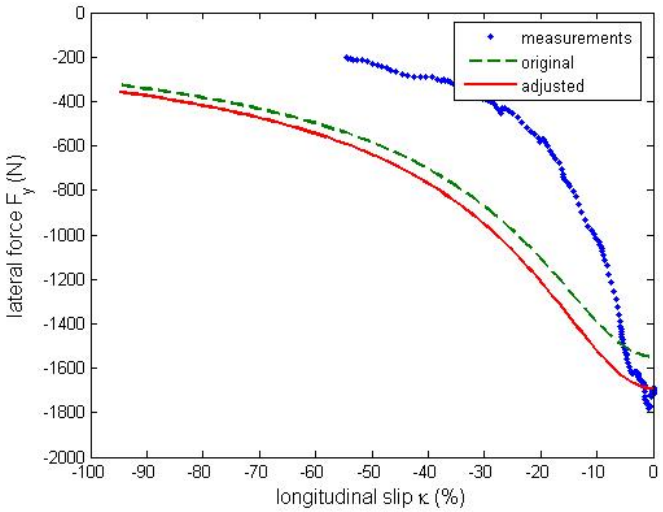

Figure 3.36: Lateral force F_{y_H}

It can be seen that changing the cornering stiffness has a big influence on the lateral force F_{y_H} in case of combined slip. In figure 3.35 this results in a better match with the measurements. In figure 3.36 this only results in a better match with the measurements from 0 to approx. -5 % longitudinal slip. Because there were no measurements with a high load and more than 3 % longitudinal slip available for the parameterization, as well as no combined measurements, the model is extrapolating for higher longitudinal slip with a high load.

3.3.3 Conclusions

It can be concluded that increasing the cornering stiffness results in a better match with the measurements. By increasing the cornering stiffness, also the stiffness of the self-aligning moment M_{z_H} and of the overturning moment M_{x_H} increases. This results in a better match with the measurements, only the extrapolation of the model for more than approx. 5 % longitudinal slip shows an increased error.

Chapter 4

Conclusions and recommendations

Within the TMPT-Benchmark a Continental tyre is considered. With the same tyre alternative tests were done at a test rig in Karlsruhe. To check the predictive behavior of the MF-Tyre/MF-Swift tyre model, several tests have been simulated in DADS with the original model parameters identified by TNO for the TMPT-Benchmark. The results of the simulations have been compared with the alternative measurements done in Karlsruhe. Now several conclusions are drawn and recommendations are made.

4.1 Conclusions

The MF-Tyre/MF-Swift tyre model is coupled to DADS. This works good and it has never crashed. The simulation speed is high, especially in case of the stationary simulations. The problems that occurred are related to the measurements, the test rig and the parameterization of the tyre model.

Stationary tests

It is a well known fact that the stationary forces and moments characteristics of a tyre can differ about 5 %, when tested on a different test rig. Therefore the difference between the original measurements and the additional measurements can be quite big.

The difference in the test rigs used for the original measurements and for the additional measurements results in several deviations. For the original measurements the curvature was not corrected. Therefore the cornering stiffness of the model is lower then that of the measurements. This has also an influence on the stiffness of the self-aligning moment, the stiffness of the overturning moment and the stiffness for the longitudinal slip. It is shown that

increasing the cornering stiffness of the model by changing the scaling factor LKY results in a better match with the measurements.

There was a great difference in the case of high loads in combination with longitudinal slip. For this case there were no measurements available for the parameterization of the tyre model. The MF-Tyre/MF-Swift tyre model is capable of making very good fits on measurements, so it is important to have a good base of measurements. The area, where no measurements have taken place, has to be checked carefully!

Dynamic tests

For the dynamic measurements the road surface of the test rig was not flat. Therefore the vertical force had a big variation. Also the reaction of the longitudinal force was in most cases not symmetric, which is unlikely.

The test rig used to simulate in DADS is a very simple model; the dynamics of the test rig were not included. For the higher speed cleat-tests the influence of the stiffness of the test rig can be big. Therefore the frequency of the simulation was higher than that of the measurements.

In the dynamic tests, the vertical force matches usually well, but the maximum of the longitudinal force was in all cleat tests too high. This is a known phenomenon of the MF-Tyre/MF-Swift model. The model can be adjusted, but that doesn't help for the predictive behavior for future studies.

4.2 Recommendations

For future investigation several recommendations can be made.

- The differences between the original measurements of the TMPT-Benchmark and the additional measurements of Karlsruhe have to be analyzed, because these differences result in several deviations between the simulations and the additional measurements.
- The test rig dynamics have to be analyzed and included in the simulations. This will result in a decrease of the frequency of the simulations, which will result in a better match with the measurements.
- In order to improve the parameterization of the model some parameters have to be fixed during the fitting process of the pure longitudinal tests and the combined tests.
- For the TMPT-Benchmark also combined measurements and measurements with high loads in combination with longitudinal slip have to be performed. Those measurements were not done and therefore the parameter identification was more difficult for those cases.

Appendix A

Pure cornering-tests

A.1 3000 N

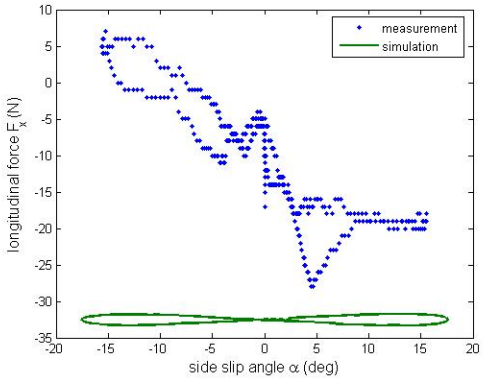

Figure A.1: Longitudinal force F_{x_H} (N)

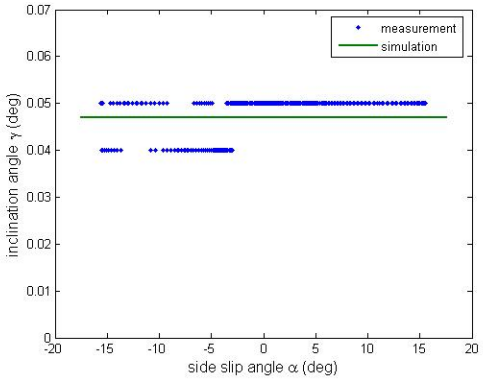

Figure A.2: Inclination angle γ (deg)

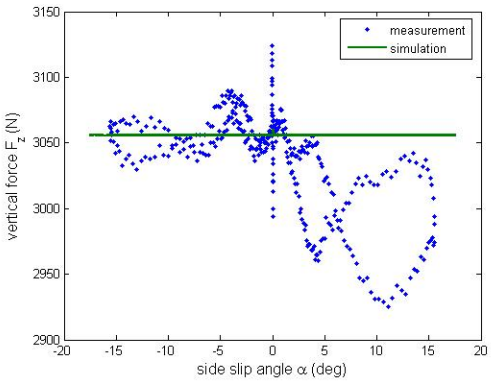

Figure A.3: Vertical force F_{z_H} (N)

A.2 6600 N

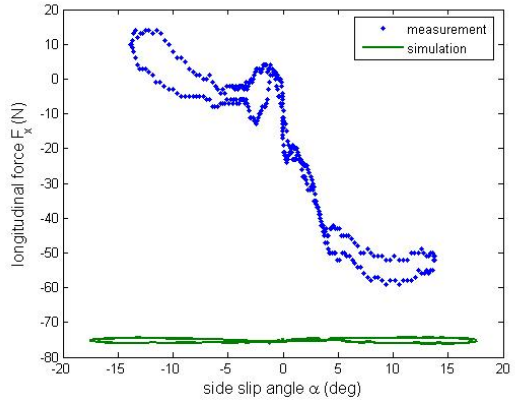

Figure A.4: Longitudinal force F_{x_H} (N)

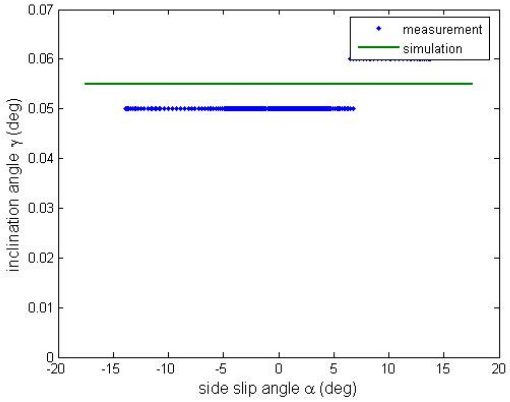

Figure A.5: Inclination angle γ (deg)

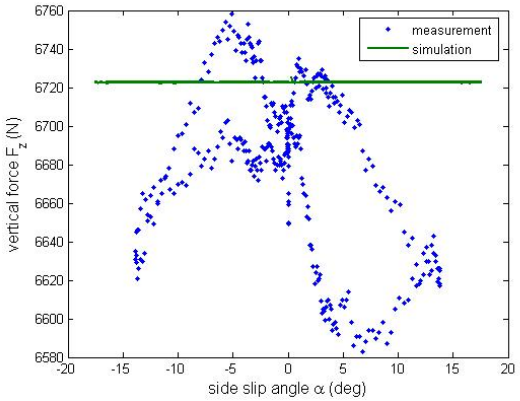

Figure A.6: Vertical force F_{z_H} (N)

Appendix B

Pure longitudinal slip-tests

B.1 3000 N

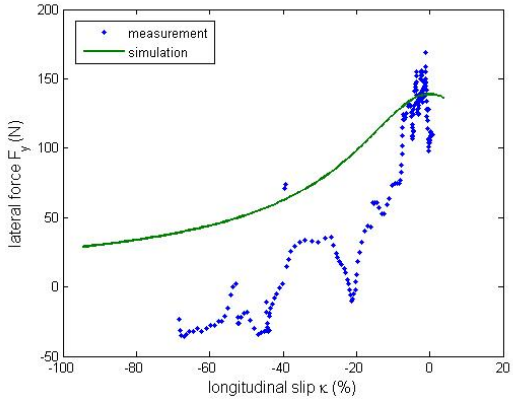

Figure B.1: Lateral force F_{y_H} (N)

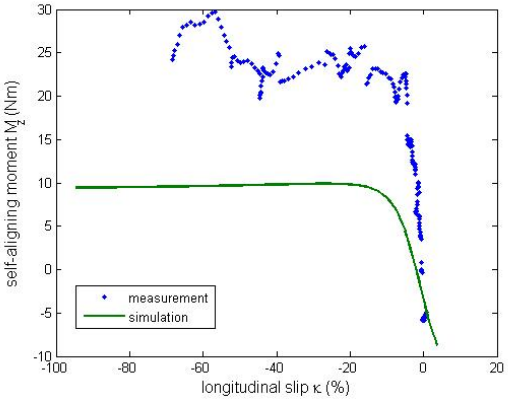

Figure B.2: Self-aligning moment M_{z_H} (Nm)

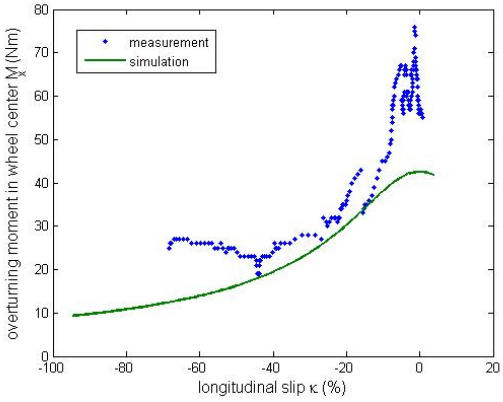

Figure B.3: Overturning moment in wheel center M_{x_H} (Nm)

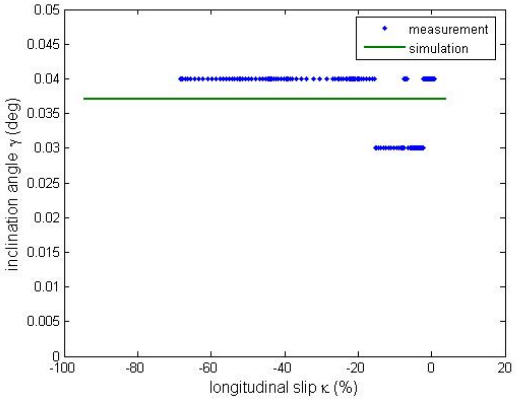

Figure B.4: Inclination angle γ (deg)

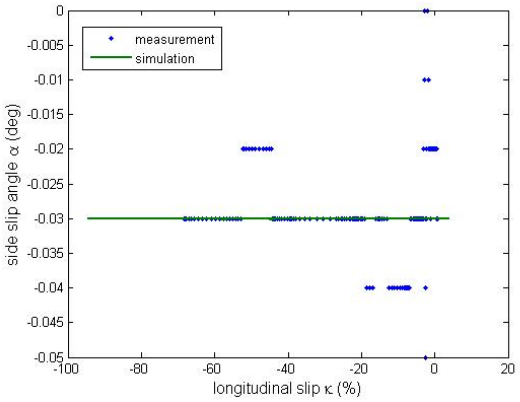

Figure B.5: Side slip angle α (deg)

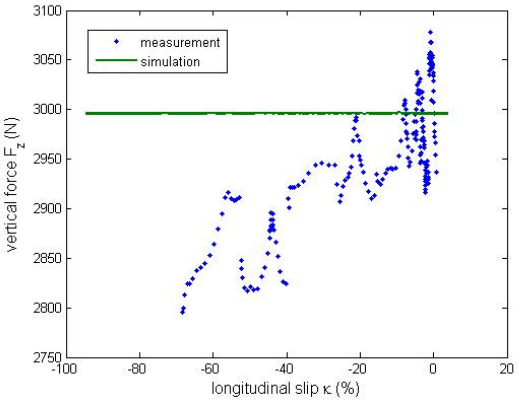

Figure B.6: Vertical force F_{z_H} (N)

B.2 6600 N

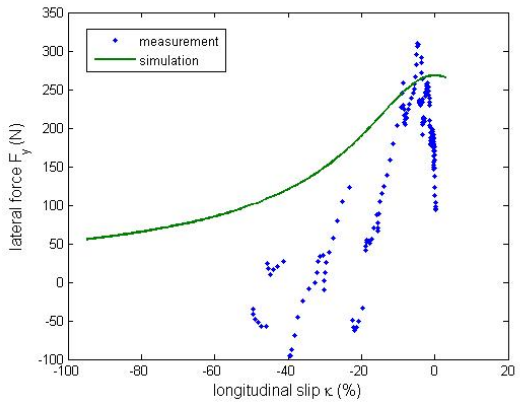

Figure B.7: Lateral force F_{y_H} (N)

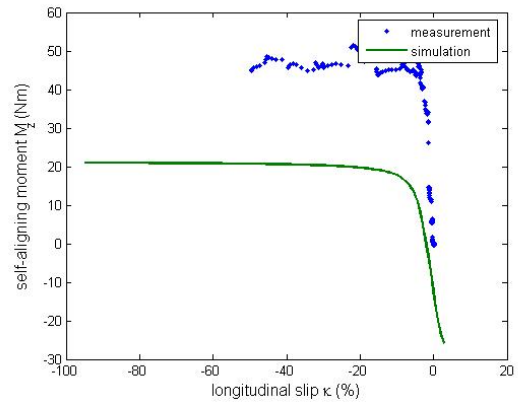

Figure B.8: Self-aligning moment M_{z_H} (Nm)

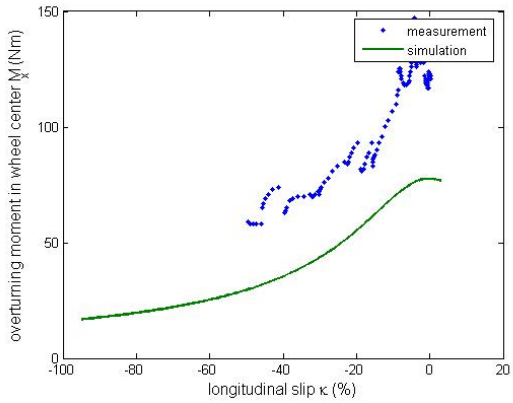

Figure B.9: Overturning moment in wheel center M_{x_H} (Nm)

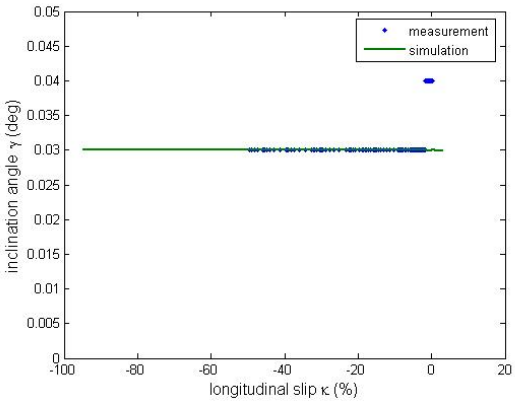

Figure B.10: Inclination angle γ (deg)

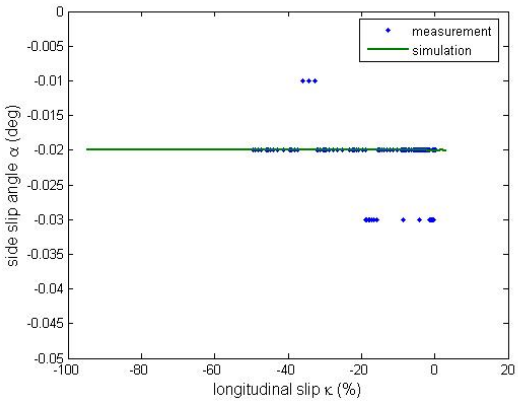

Figure B.11: Side slip angle α (deg)

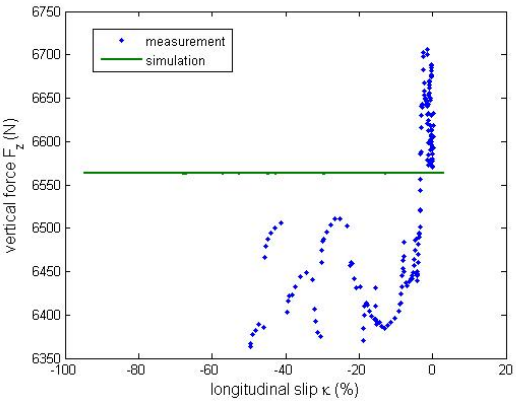

Figure B.12: Vertical force F_{z_H} (N)

Appendix C

Combined slip-tests

C.1 3000 N

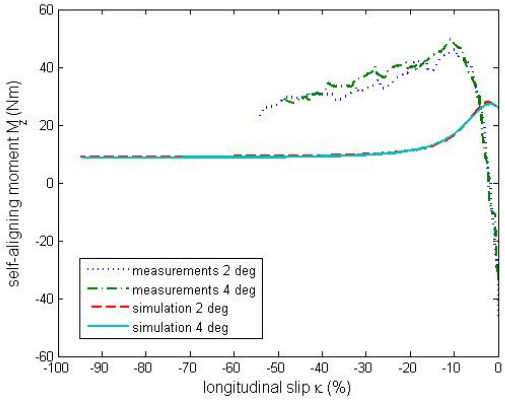

Figure C.1: Self-aligning moment M_{z_H} (Nm)

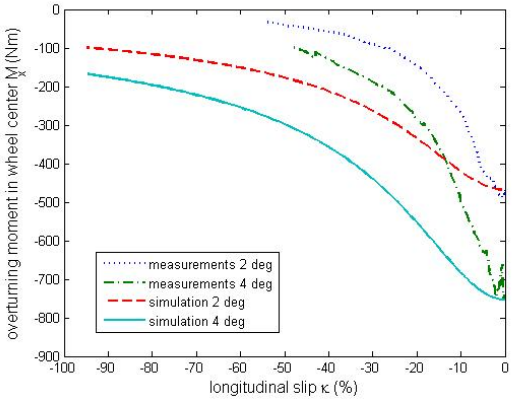

Figure C.2: Overturning moment in wheel center M_{x_H} (Nm)

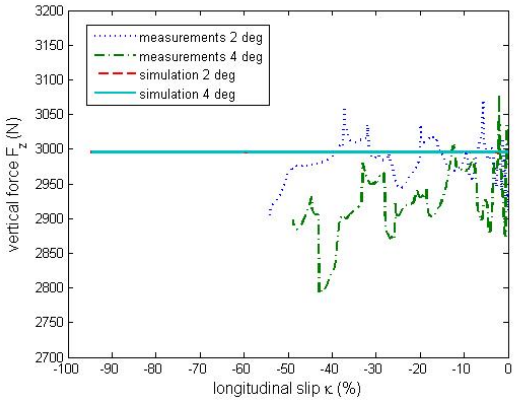

Figure C.3: Vertical force F_{z_H} (N)

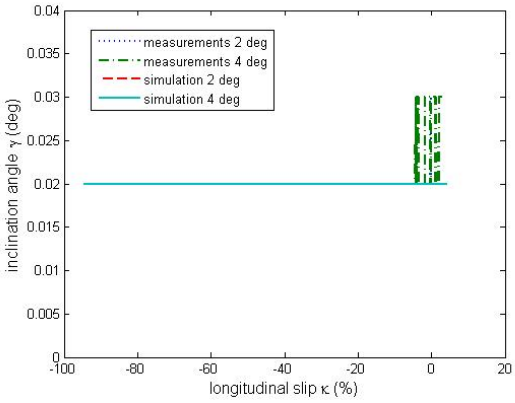

Figure C.4: Inclination angle γ (deg)

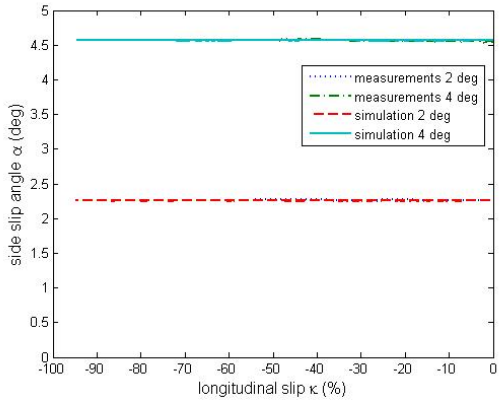

Figure C.5: Side slip angle α (deg)

C.2 6600 N

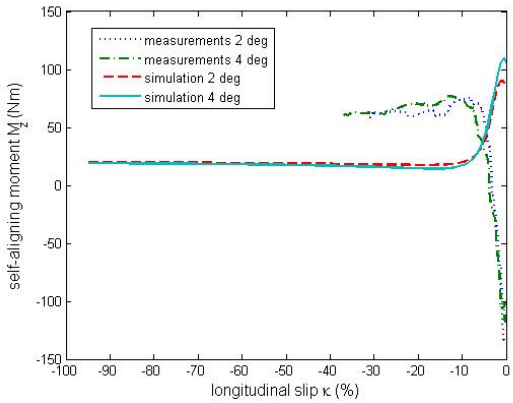

Figure C.6: Self-aligning moment M_{z_H} (Nm)

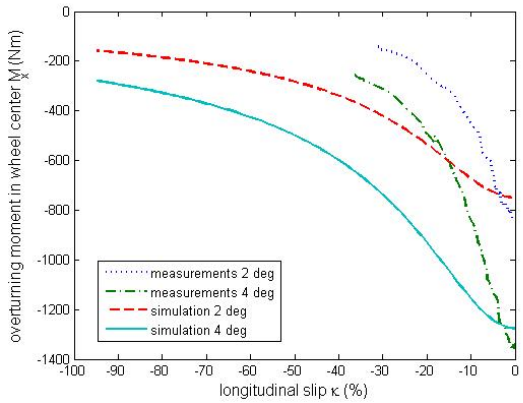

Figure C.7: Overturning moment in wheel center M_{x_H} (Nm)

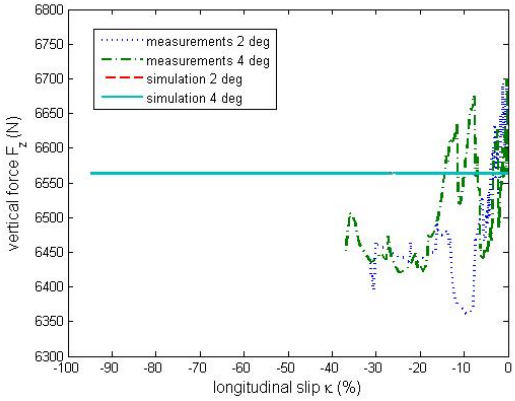

Figure C.8: Vertical force F_{z_H} (N)

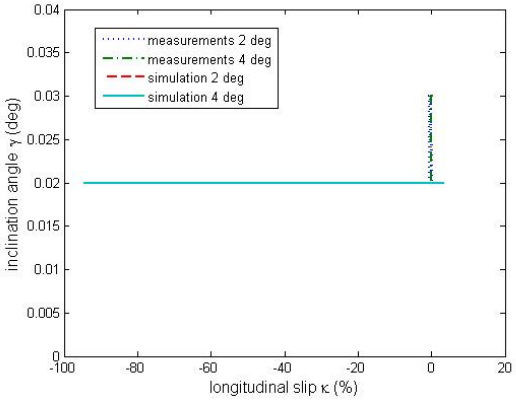

Figure C.9: Inclination angle γ (deg)

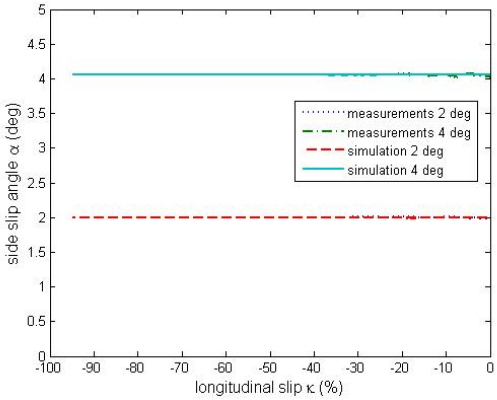

Figure C.10: Side slip angle α (deg)

Appendix D

30 mm cleat-tests

D.1 Wheel center height resulting in a load of 1700 N

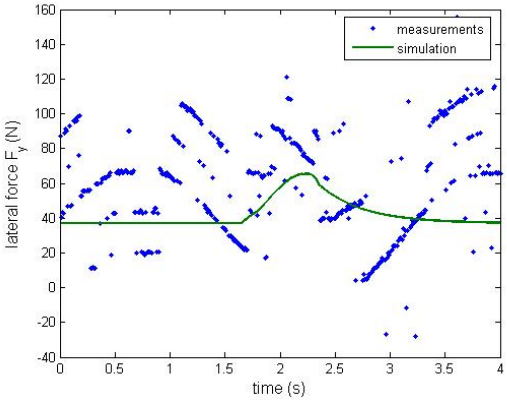

Figure D.1: Lateral force F_{y_C} (N)

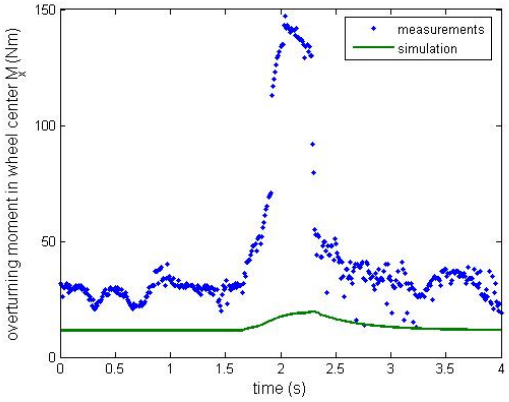

Figure D.2: Overturning moment in wheel center M_{x_C} (Nm)

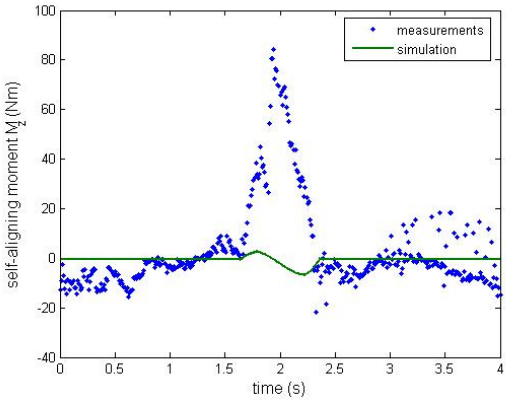

Figure D.3: Self-aligning moment M_{z_C} (Nm)

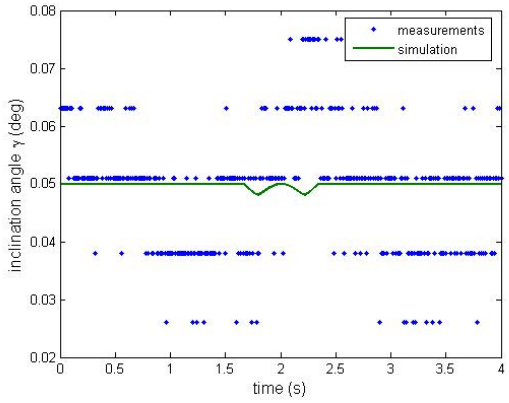

Figure D.4: Inclination angle γ (deg)

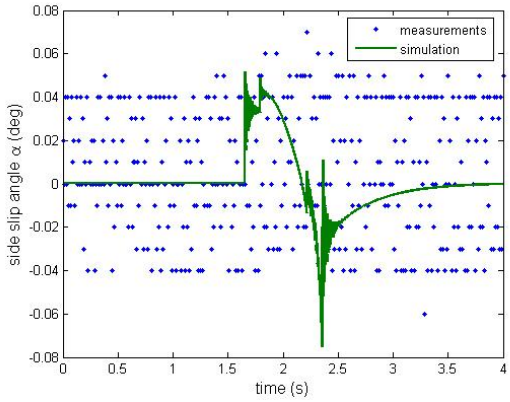

Figure D.5: Side slip angle α (deg)

D.2 Wheel center height resulting in a load of 4800 N

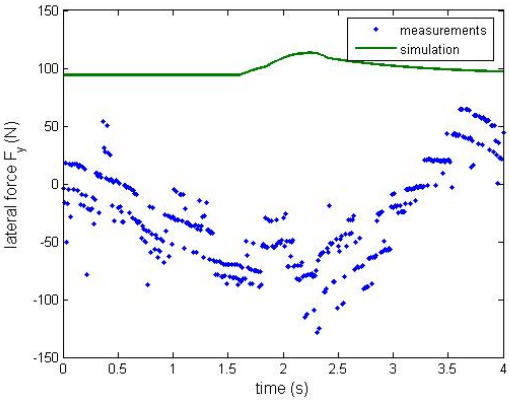

Figure D.6: Lateral force F_{y_C} (N)

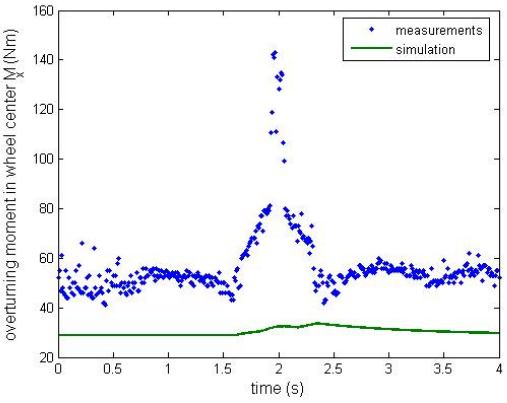

Figure D.7: Overturning moment in wheel center M_{x_C} (Nm)

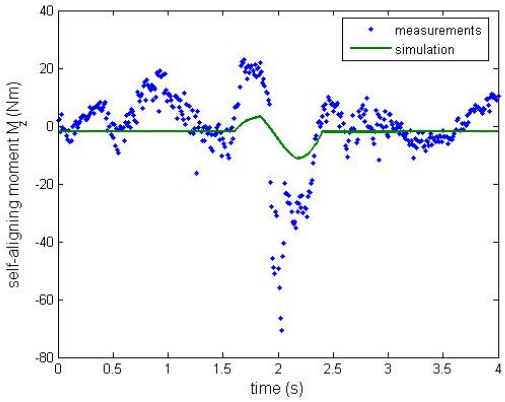

Figure D.8: Self-aligning moment M_{zC} (Nm)

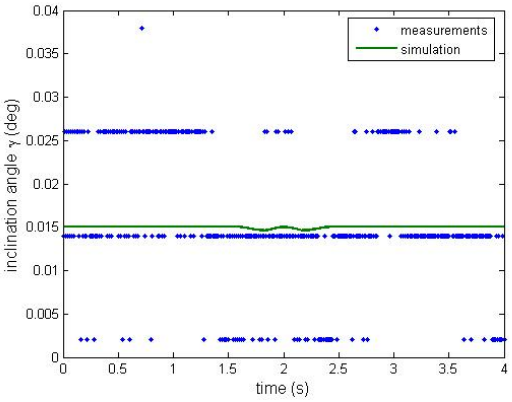

Figure D.9: Inclination angle γ (deg)

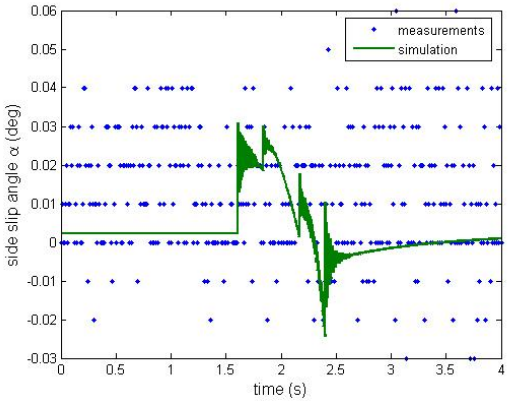

Figure D.10: Side slip angle α (deg)

Appendix E

10 mm cleat-tests with 2 km/h

E.1 Wheel center height resulting in a load of 1700 N

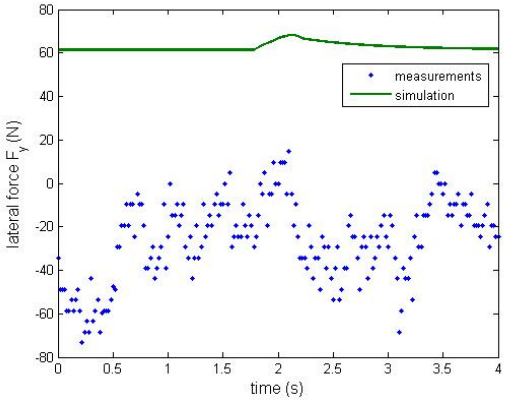

Figure E.1: Lateral force F_{y_C} (N)

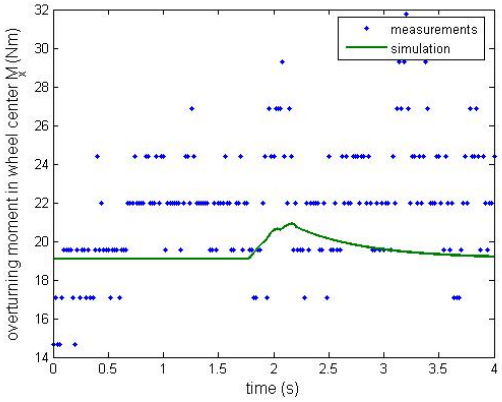

Figure E.2: Overturning moment in wheel center M_{x_C} (Nm)

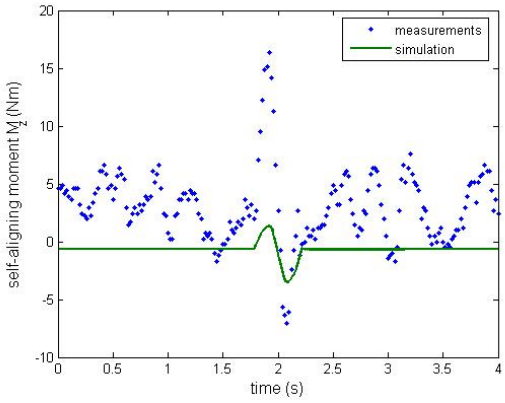

Figure E.3: Self-aligning moment M_{z_C} (Nm)

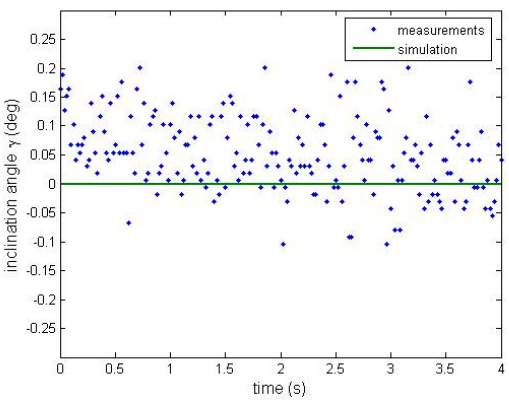

Figure E.4: Inclination angle γ (deg)

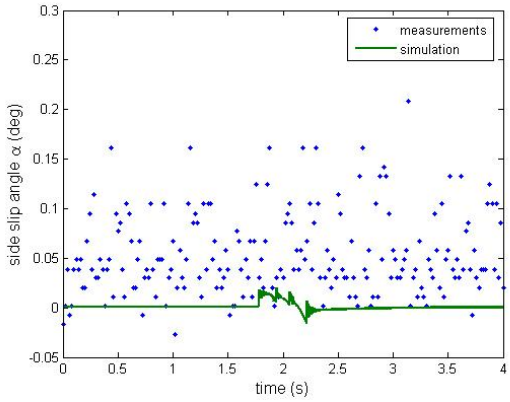

Figure E.5: Side slip angle α (deg)

E.2 Wheel center height resulting in a load of 4800 N

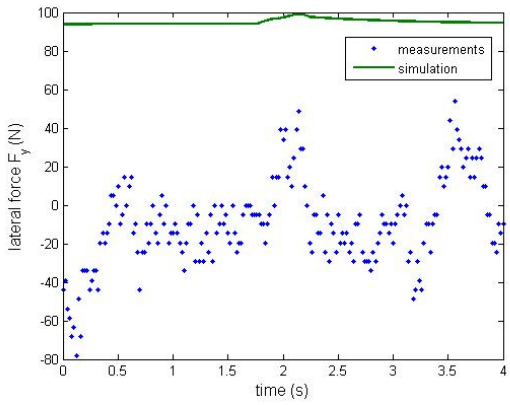

Figure E.6: Lateral force F_{y_C} (N)

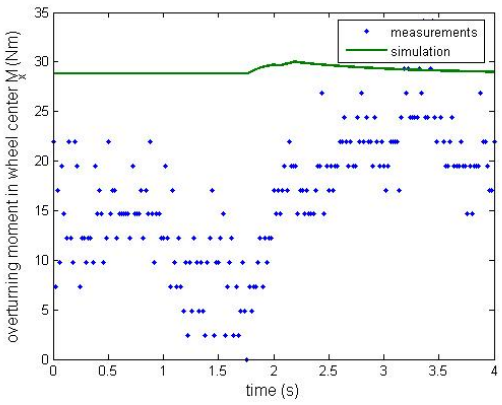

Figure E.7: Overturning moment in wheel center M_{x_C} (Nm)

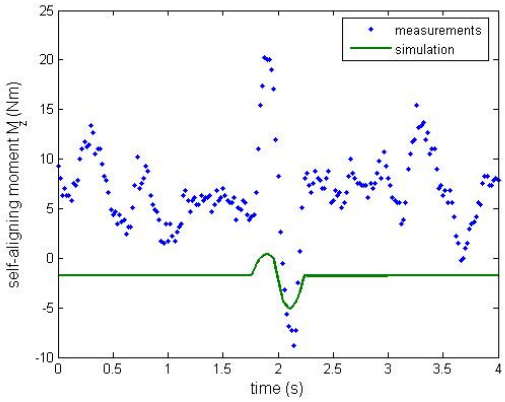

Figure E.8: Self-aligning moment M_{zC} (Nm)

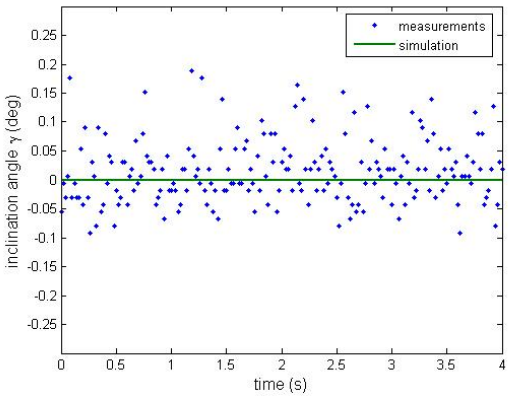

Figure E.9: Inclination angle γ (deg)

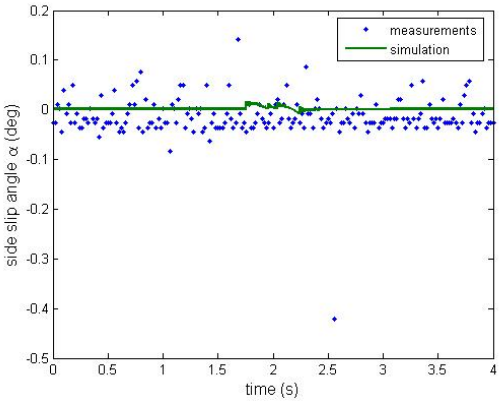

Figure E.10: Side slip angle α (deg)

Appendix F

10 mm cleat-tests with 30 km/h

F.1 Wheel center height resulting in a load of 1700 N

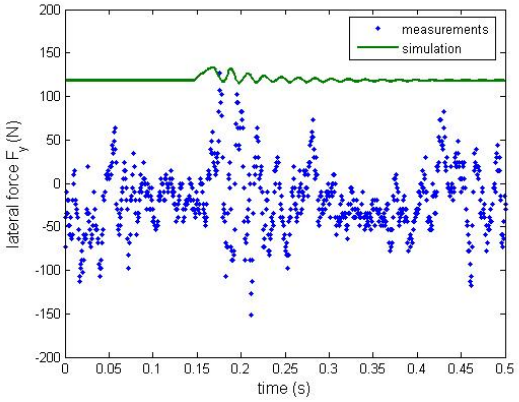

Figure F.1: Lateral force F_{y_C} (N)

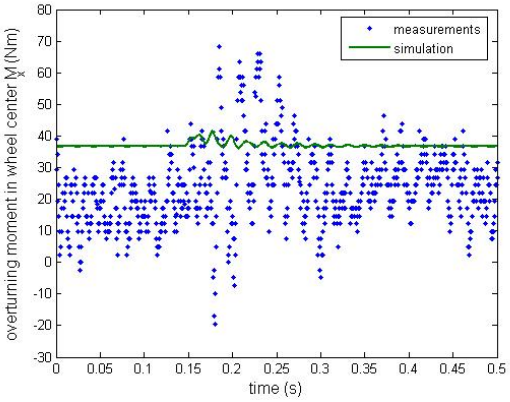

Figure F.2: Overturning moment in wheel center M_{x_C} (Nm)

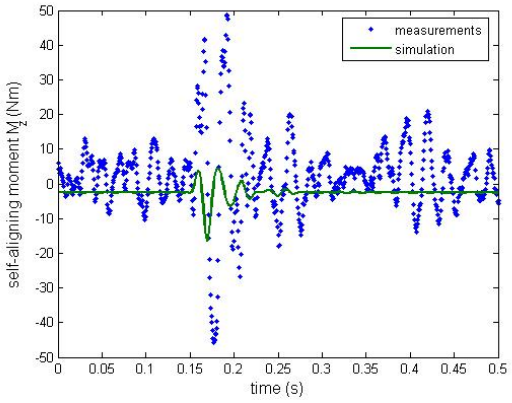

Figure F.3: Self-aligning moment M_{z_C} (Nm)

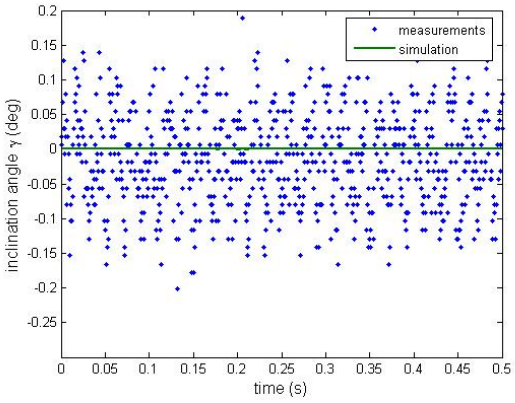

Figure F.4: Inclination angle γ (deg)

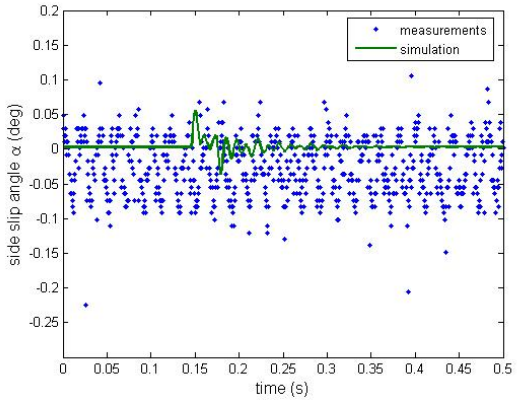

Figure F.5: Side slip angle α (deg)

F.2 Wheel center height resulting in a load of 4800 N

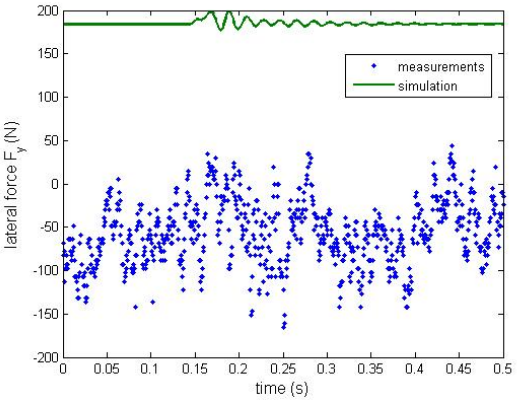

Figure F.6: Lateral force F_{y_C} (N)

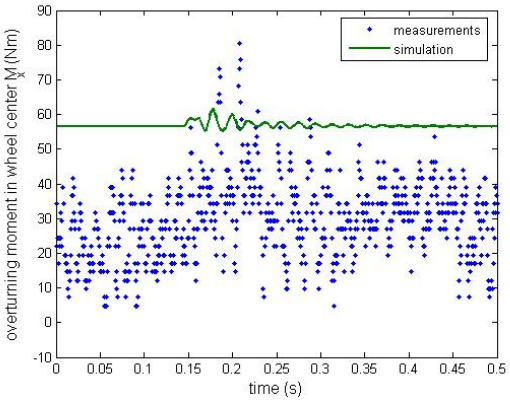

Figure F.7: Overturning moment in wheel center M_{x_C} (Nm)

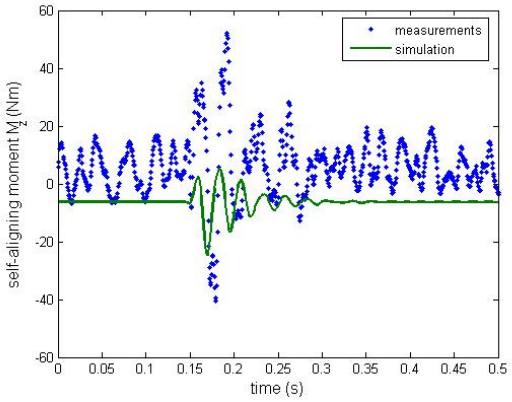

Figure F.8: Self-aligning moment M_{zC} (Nm)

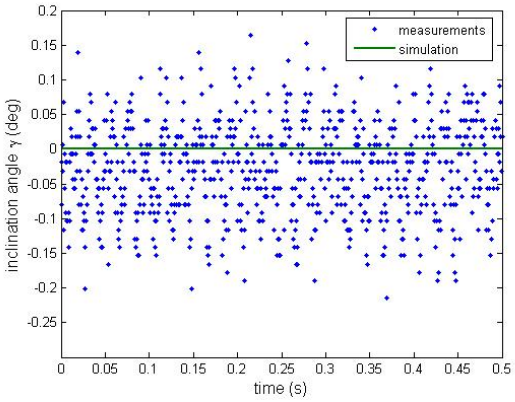

Figure F.9: Inclination angle γ (deg)

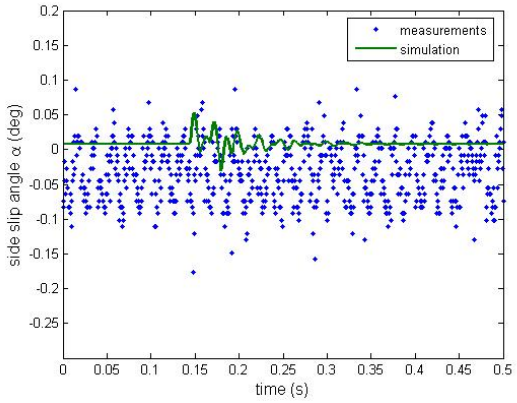

Figure F.10: Side slip angle α (deg)

References

[1] Besselink, I.J.M. et Al.
The Swift tyre model: overview and applications. Paper 'Proceedings of the International symposium on Advanced Vehicle Control 2004', page 525-530

[2] Gnadler, R.
Erläuterungen zu den Messungen mit dem Reifen Continental 205/55 R16 90H (PCI-S) aus dem TMPT-Benchmark. PDF document Karlsruhe: University of Karlsruhe, 2005

[3] TNO Automotive
MF-Tyre/MF-Swift 6.0 Installation Instructions.
Helmond: TNO Automotive, 2004

[4] TNO Automotive
MF-Tyre/MF-Swift 6.0 Tutorial. PDF document.
Helmond: TNO Automotive, 2004